Transcriptional Analysis in the Arabidopsis Roots Reveals New Regulators that Link rac-GR24 Treatment with Changes in Flavonol Accumulation, Root Hair Elongation and Lateral Root Density

Sylwia Struk, Lukas Braem, Cedrick Matthys, Alan Walton, Nick Vangheluwe, Stan van Praet, Lingxiang Jiang, Pawel Baster, Carolien de Cuyper, François-Didier Boyer, et al.

Transcriptional Analysis in the Arabidopsis Roots Reveals New Regulators that Link *rac*-GR24 Treatment with Changes in Flavonol Accumulation, Root Hair Elongation, and Lateral Root Density

Running title: Transcriptional responses to *rac*-GR24 in the root

Corresponding author:

S. Goormachtig

VIB-UGent Center for Systems Biology

Technologiepark 71

9052 Gent

Belgium

Tel. +32 9 3313 910; Fax +3é 9 3313 809

E-mail: Sofie.goormachtig@psb.vib-ugent.be

Subject Area:

Growth and development

Figures: 1 (black & white), 6 (color)

Tables: 0

SI file: 1

Transcriptional Analysis in the Arabidopsis Roots Reveals New Regulators that Link *rac*-GR24 Treatment with Changes in Flavonol Accumulation, Root Hair Elongation, and Lateral Root Density

Sylwia Struk,[1,2] Lukas Braem,[1,2,3,4] Cedrick Matthys,[1,2] Alan Walton,[1,2,3,4] Nick Vangheluwe,[1,2] Stan Van Praet,[1,2,5] Lingxiang Jiang,[1,2] Pawel Baster,[1,2] Carolien De Cuyper,[1,2] François-Didier Boyer,[6,7] Elisabeth Stes,[1,2,3,4] Tom Beeckman,[1,2] Jiří Friml,[1,2,8] Kris Gevaert,[3,4] and Sofie Goormachtig[1,2*]

0000-0002-9481-4333 (S.S.), 0000-0002-4885-6161 (N.V.), 0000-0002-5169-1054 (S.V.P.), 0000-0003-1794-0755 (L.J.), 0000-0002-8098-8703 (C.D.C.), 0000-0001-9855-7234 (F.-D.B.), 0000-0001-8656-2060 (T.B.), 0000-0002-8302-7596 (J.F.), 0000-0002-4237-0283 (K.G.), 0000-0001-6195-9889 (S.G.)

[1] Department of Plant Biotechnology and Bioinformatics, Ghent University, 9052 Ghent, Belgium

[2] Center of Plant Systems Biology, VIB, 9052 Ghent, Belgium

[3] Department of Biomolecular Medicine, Ghent University, 9000 Ghent, Belgium

[4] Center for Medical Biotechnology, VIB, 9000 Ghent, Belgium

[5] Laboratory of Plant Growth Analysis, Ghent University Global Campus, Incheon 21985, Republic of Korea

[6] Institut Jean-Pierre Bourgin, Institut National de la Recherche Agronomique, AgroParisTech, Centre National de la Recherche Scientifique, Université Paris-Saclay, 78026 Versailles, France

[7]Institut de Chimie des Substances Naturelles, Centre National de la Recherche Scientifique, UPR2301, Université Paris-Sud, Université Paris-Saclay, 91198 Gif-sur-Yvette, France

[8] Institute of Science and Technology (IST) Austria, 3400 Klosterneuburg, Austria

* Corresponding author: E-mail, sofie.goormachtig@psb.vib-ugent.be; Fax, +32 9 3313809

Abstract

The synthetic strigolactone (SL) analog, *rac*-GR24, has been instrumental in studying the role of SLs as well as karrikins, because it activates the receptors DWARF14 (D14) and KARRIKIN INSENSITIVE2 (KAI2) of their signaling pathways, respectively. Treatment with *rac*-GR24 modifies the root architecture at different levels, such as decreasing the lateral root density (LRD), while promoting root hair elongation or flavonol accumulation. Previously, we have shown that the flavonol biosynthesis is transcriptionally activated in the root by *rac*-GR24 treatment, but, thus far, the molecular players involved in that response have remained unknown. To get an in-depth insight into the changes that occur after the compound is perceived by the roots, we compared the root transcriptome of wild-type and the *more axillary growth2* (*max2*) mutant, affected in both SL and karrikin signaling pathways, with and without *rac*-GR24 treatment. qRT-PCR, reporter line analysis, and mutant phenotyping indicated that the flavonol response and the root hair elongation are controlled by the ELONGATED HYPOCOTYL5 (HY5) and MYB12 transcription factors, but HY5, in contrast to MYB12, affects the LRD as well. Furthermore, we identified the transcription factors TARGET OF MONOPTEROS5 (TMO5) and TMO5-LIKE1 as negative and the Mediator complex as positive regulators of the *rac*-GR24 effect on LRD. Altogether, hereby, we get closer toward understanding the molecular mechanisms that underlay the *rac*-GR24 responses in the root.

Keywords Flavonols • MAX2 • *rac*-GR24 • RNA-seq • Root development • Transcriptional regulation

Accession numbers

The ATG codes of the different mutants used in this study were: AT3G03990 (D14), AT4G37470 (KAI2), AT2G42620 (MAX2), AT5G13930 (CHS), AT2G47460 (MYB12), AT5G11260 (HY5), AT1G25540 (PFT1), AT3G25710 (TMO5) and AT1G68810 (TMO5L1).

Introduction

Strigolactones (SLs) are carotenoid-derived compounds that act as plant hormones in various developmental processes and that are exuded in the rhizosphere, inducing parasitic plant germination and initiating arbuscular mycorrhization (Cook et al. 1966; Akiyama et al. 2005; Kobae et al. 2018). In the canonical SL pathway, the F-box protein MORE AXILLARY GROWTH 2 (MAX2) forms a complex with the SL receptor DWARF14 (D14) in the presence of SLs, resulting in the ubiquitination and subsequent degradation of their targets SUPPRESSOR OF MAX2 (SMAX1) LIKE6 (SMXL6), SMXL7, and SMXL8 (designated SMXL6,7,8 throughout) (Stanga et al. 2013; Soundappan et al. 2015; Wang et al. 2015; Liang et al. 2016). MAX2 is also recruited in the signaling pathway of karrikins (KARs), i.e., smoke-derived compounds involved in germination (Nelson et al. 2011). These KARs bind to another α/β fold hydrolase that is a close relative of D14, namely KARRIKIN INSENSITIVE 2 (KAI2) (Guo et al. 2013). Upon KAR treatment, SMAX1 and SMXL2, homologs of SMXL6,7,8, are ubiquitinated and degraded in a MAX2- and KAI2- dependent manner (Stanga et al. 2013, 2016; Khosla et al. 2020). Because of the phenotypic defects observed in the *kai2* mutant, the KAR receptor is thought to perceive also a yet unknown endogenous molecule, designated as KAI2-ligand (KL) (Conn and Nelson 2016).

Whereas the SL and KAR/KL pathways are mostly active in different developmental processes, some responses have been reported to be controlled by both. For instance, the *max2* mutants present belowground phenotypes, such as an increased lateral root density (LRD) under control conditions and insensitivity to the synthetic SL analog *rac*-GR24–induced root hair elongation and LRD reduction (Kapulnik et al. 2011a, 2011b; Villaécija-Aguilar et al. 2019). These effects were shown to depend on *KAI2* and *D14* and to be complemented by *smxl6,7,8* and *smax1*/*smxl2*, indicating that both pathways govern this response (Soundappan et al. 2015; Wang et al. 2015; Villaécija-Aguilar et al. 2019). Additionally, recently, some interconnection has been suggested at the molecular level regarding the receptor–target interaction in response to exogenous ligands. Indeed, degradation of SMXL2 can be triggered by both D14 and KAI2 receptors after perception of the SL and KAR ligands, respectively, to control seedling photomorphogenesis and downstream gene expression (Wang et al. 2020a). Also, the KAI2-SMXL6/7/8 interaction has been proposed to regulate the skewing angle of the roots (Swarbreck et al. 2019) and the development of adventitious roots at the root–shoot junction in *Arabidopsis thaliana* (Swarbreck et al. 2020).

Beyond the study of the endogenous effects through genetic analysis, the field has also greatly benefited from the development of synthetic SL analogs, such as *rac*-GR24 (Bergmann et al. 1993). Application of this compound rescued the defects of the SL biosynthesis mutants and influenced the root system architecture by increasing the primary root length, due to size enhancement of the meristem and the transition zone (Ruyter-Spira et al. 2011). Additionally, when plants were grown under nutrient-rich conditions, treatment with *rac*-GR24 led to an increase in root hair length and a MAX2-dependent reduction in LRD (Kapulnik et al. 2011a; Ruyter-Spira et al. 2011; Kapulnik and Koltai 2014; De Cuyper et al. 2017), the latter depending on auxin (Ruyter-Spira et al. 2011) and largely affecting the lateral root emergence in the upper root part (Jiang et al. 2016).

Although significant insights have been obtained into the SL signaling in the past decade, many downstream molecular players are still largely unknown (Soundappan et al. 2015; Wang et al. 2015; Bennett et

al. 2016; Liang et al. 2016). Transcription-dependent, as well as transcription-independent, signaling mechanisms have been proposed (Shinohara et al. 2013; Liang et al. 2016, Wang et al. 2020b; Zhang et al. 2020). Recent transcriptomic analysis with the SL enantiomer $GR24^{4DO}$ that specifically activates D14 signaling revealed that SLs control shoot branching, leaf development, and anthocyanin biosynthesis mainly through transcriptional activation of the BRANCHED 1 (BRC1), TCP DOMAIN PROTEIN 1 (TCP1), and PRODUCTION OF ANTHOCYANIN PIGMENT 1 (PAP1), respectively (Wang et al. 2020b). Nevertheless, the transcriptional regulation of other aspects of plant development by SL and KAR/KL remained to be uncovered. An unbiased forward genetics screen for mutants with a *rac*-GR24–insensitive root growth hinted at the role of the Mediator complex (Baster 2014). This complex is known to control transcription at the RNA polymerase II assembly level and through the regulation of chromatin remodeling (Kagey et al. 2010), suggesting the involvement of the transcription- dependent mechanisms in *rac*-GR24 related root phenotypes.

Production of flavonols has also been linked to SL and KAR responses. Inside the root tissue, the flavonol accumulation is activated by *rac*-GR24, or any of its enantiomers, depending on MAX2 and the two receptors D14 and/or KAI2 as well. A proteome analysis of Arabidopsis Columbia-0 (Col-0) accession and *max2* mutants treated with *rac*-GR24 further revealed changes in protein abundance of enzymes involved in different steps of the flavonoid biosynthesis. Indeed, a MAX2-dependent increase in protein abundance of PHENYLALANINE AMMONIA LYASE 1 (PAL1), CFI family protein, and FLAVANONE 3'-HYDROXYLASE (F3'H) was detected in response to *rac*-GR24, whereas other proteins, including PAL2, FLAVANOL SYNTHASE 1 (FLS1), CHALCONE SYNTHASE (CHS), and UDP-GLUCOSYL TRANSFERASE 78D2 (UGT78D2) were significantly more abundant in the wild-type than in the *max2* roots under control conditions. Accordingly, the transcript levels of genes encoding several of these enzymes were upregulated upon *rac*-GR24 treatment in a MAX2-dependent manner, but the molecular network that connects *rac*-GR24 signaling with the transcriptional changes remained elusive (Walton et al. 2016).

Flavonols are a subgroup of phenolic compounds that modulate plant growth, development and stress responses (Taylor and Grotewold 2005) and might possibly negatively regulate root growth, as well as the development of lateral roots and root hairs. Two non-exclusive mechanisms have been proposed to explain this process (Silva-Navas et al. 2016). Firstly, flavonols act as negative regulators of the polar auxin transport and distribution (Lewis et al., 2011; Grunewald et al., 2012; Tan et al., 2019) and secondly, by their antioxidant capability, flavonols modulate Reactive Oxygen Species (ROS) accumulation (Gayomba et al. 2017; Gayomba and Muday 2020; Chapman and Muday 2021). The biosynthesis of flavonols is directly controlled at least by three MYB transcription factors, MYB11, MYB12, and MYB111 (Mehrtens et al. 2005, Stracke et al., 2007, 2010a; Zhang et al., 2021). Several factors have been described that regulate the activity of MYBs, including ELONGATED HYPOCOTYL 5 (HY5) and CONSTITUTIVE PHOTOMORPHOGENIC 1 (COP1) in response to visible and UV-B light (Stracke et al. 2010b; Bhatia et al. 2021). In addition, the plant hormones auxin and ethylene transcriptionally activate *MYB12,* inducing flavonol accumulation in the root in a TRANSPORT INHIBITOR RESPONSE 1 (TIR1)- and ETHYLENE INSENSITIVE 2 (EIN2)-dependent manner, respectively (Lewis et al., 2011). By contrast, gibberellic acid (GA) was shown to regulate root growth by reducing the flavonol accumulation, as the interaction of DELLA proteins with MYB12 and MYB111 enhances their binding to the promoter regions of key flavonol biosynthesis genes (Tan et al. 2019).

Taking into account the diverse physiological effects that are attributed to *rac*-GR24 in the *Arabidopsis* root, we can assume that they are coordinated by various transcriptional networks that are controlled by both the D14 and KAI2 pathways. As no detailed insights in the *rac*-GR24 transcriptional responses in the root were available, we carried out a transcriptome study. Here, we describe several new transcriptional regulators that are differentially expressed in *rac*-GR24–treated roots and demonstrate their role by using mutants and marker lines.

Results

rac-*GR24 influence on the transcriptome of the wild-type and max2 roots*

Recently, several key SL-responsive genes have been shown to regulate shoot branching, leaf development, anthocyanin accumulation, and drought adaption (Wang et al. 2020b). The identification of the Mediator complex suggested that transcriptional players might also be involved in *rac*-GR24–induced root phenotypes. To confirm the role of the Mediator-mediated transcriptional regulation in the impact of *rac*-GR24 in roots, we investigated the *protein farnesyltransferase1-2* (*pft1-2*) and *pft1-3* mutant alleles defective in the Mediator function. Both *pft1-2* and *pft1-3* did not display an increased LRD phenotype under mock conditions, but were significantly less sensitive to the *rac*-GR24 treatment than the wild-type (WT) plants (P <0.001, Poisson regression model) (Supplementary Fig. S1). Hence, these data imply that transcriptional changes are indeed important for the effect provoked by exogenous *rac*-GR24 in roots.

To discover the transcriptional targets controlling *rac*-GR24-dependent responses in the root, we carried out an RNA-sequence (RNA-seq) experiment on Col-0 and *max2* mutant plants treated with either 1 µM *rac*-GR24 or 0.01% (v/v) acetone (mock) for 6 h. This 6-h time point had been selected based on previous studies and marker genes (Walton et al. 2016). To enrich for statistically and biologically significant differentially expressed genes, we applied two selection criteria, namely a corrected P value (False Discovery Rate, FDR) < 0.05 and a fold change (FC) cutoff of either 1.2 or 0.83. For *rac*-GR24–treated WT plants, 146 differentially expressed genes were identified, of which 63 were induced and 83 were repressed (Supplementary Dataset S1). The comparison between *max2* and WT seedlings grown under mock conditions resulted in 2,011 differentially expressed genes, of which 882 were upregulated and 1,129 were downregulated (Supplementary Dataset S2). After *rac*-GR24 treatment of *max2* roots, 107 differentially expressed genes were detected, of which 87 were upregulated and 20 downregulated (Supplementary Dataset S3). All unique and overlapping differentially expressed genes (Supplementary Datasets S1-S3) were determined and are presented as UpSet plot (Fig. 1, Supplementary Datasets S4). The qRT-PCR analysis confirmed differential expression of three out of seven selected candidate genes (AT1G60750, AT3G54530 and AT4G28850), indicating that some *rac*-GR24–induced transcriptional changes might be independent of *MAX2* (Supplementary Fig. S2).

When the dataset of genes differentially expressed between *max2* and WT under mock conditions was compared with the root proteome analysis carried out for the same genotypes, 57 common candidates were found (Supplementary Table S1). With the exception of three genes, the proteomic profile was similar to the transcriptional one, indicating that the transcriptional changes might contribute to the observed modifications in the proteome (Walton et al. 2016). Recently, the SL analog, $GR24^{4DO}$ has been shown to specifically act through D14 to activate the SL signaling in *Arabidopsis* seedlings and treatment with this compound allowed the

identification of 401 SL-responsive genes (Wang et al. 2020b). As *rac*-GR24 used here stimulates both the SL and KAR signaling (Scaffidi et al. 2014) and both pathways are known to be involved in root development (Villaécija-Aguilar et al. 2019), we compared both datasets to search for SL-specific transcriptional responses in the root. The comparison of genes differentially expressed after *rac*-GR24 treatment in Col-0, but not in *max2* root tissue, and $GR24^{4DO}$-treated Col-0 seedlings (Wang et al. 2020b) resulted in 11 common candidates (AT4G21760/Beta-glucosidase 47; AT5G03680/Duplicated homeodomain-like superfamily protein; AT2G22590/UDP-Glycosyltransferase superfamily protein; AT1G03840/C2H2 and C2HC zinc fingers superfamily protein; AT5G07990/Cytochrome P450 superfamily protein; AT1G28110/Serine carboxypeptidase-like 45; AT4G30350/SMXL2; AT4G36670/Major facilitator superfamily protein; AT4G39675/Hypothetical protein; AT5G53980/Homeobox protein 52; and AT5G19890/Peroxidase superfamily protein; Supplementary Table S2), suggesting that these genes might be specific for SL responses in the root. Finally, in search for genes that might act in the root downstream of the KAI2 pathway, we compared our data with a recently published transcriptome of red light-grown *smax1 smxl2* seedlings (Bursch et al. 2021). We found 95 genes that were downregulated in *max2* while upregulated in *smax1 smxl2* seedlings when compared to the wild type (Supplementary Dataset S5). Although very distinct experimental conditions had been used to generate the transcriptomics datasets, the results might give a hint which genes are exclusively involved in SL or KAR/KL pathways in the root.

Expression of the KAI2 *and* D14 *signaling components in the roots of mutants and upon treatment with* rac-*GR24*

Further analysis of possible changes in the gene expression of known components involved in *rac*-GR24 signaling did not reveal any expression modifications in either *D14, KAI2*, or *MAX2* in any comparison (Supplementary Datasets S1-S3). In contrast, two of the SMAX1/SMXL clade, *SMXL2* and *SMXL7*, were upregulated in the WT after the *rac*-GR24 treatment and the expression of *SMAX1*, *SMXL2*, and *SMXL7* under mock conditions was lower in the roots of the *max2* mutant than that of WT (Fig. 2A).

To confirm these observations, we evaluated the expression of these genes by qRT-PCR in WT roots after mock treatment and with *rac*-GR24 for 6 and 24 h. The expression of the three genes was significantly induced after 24 h of *rac*-GR24 treatment, but no difference was detected after 6 h (Fig. 2B). Analysis of *SMXL2* and *SMXL7* GUS reporter lines revealed increased expression after treatment with *rac*-GR24 for both constructs. For *SMXL7*, the blue staining was intensified in the vascular tissue of the hypocotyl and in the older root parts, whereas for *SMXL2* in the vascular tissue of the root elongation zone and at the basis of newly formed lateral roots (Supplementary Figs S3 and S4).

Next, the expression levels of *SMAX1*, *SMXL2*, and *SMXL7* were analyzed in the roots of *d14*, *kai2*, *d14;kai2,* and *max2* mutants. The expression of *SMAX1* and *SMXL2* was significantly reduced in *kai2*, *d14;kai2,* and *max2* in agreement with the signaling pathway in which they act. The transcript level of *SMXL7* was slightly, but not significantly reduced in either mutant (Fig. 2C).

Altogether, by means of qRT-PCR and GUS reporter lines, we confirmed the data obtained by RNA-seq, demonstrating that treatment with *rac*-GR24 increased the expression of *SMAX1, SMXL2*, and *SMXL7*. Under mock conditions, the expression levels of *SMAX1,* and *SMXL*2 in the root seemed to be controlled solely by the

KAI2 receptor. Based on our analysis it is difficult to conclude which of the receptors is required for the regulation of the *SMXL7* transcript levels.

Expression of flavonol biosynthesis genes is controlled by both D14 and KAI2

Our previous proteome study had revealed that, for at least for five proteins related to the phenylpropanoid pathway, the accumulation levels were lower in the *max2-1* mutant than in the WT. In agreement, their expression at protein level was upregulated in Col-0 roots upon treatment with *rac*-GR24 or any of its enantiomers (Walton et al. 2016). Additionally, we had demonstrated that the origin could be ascribed to transcriptional changes, because the expression of *PAL1*, *FLS1,* and *CHS* genes*,* among others, was induced after 24 h of *rac*-GR24 treatment (Walton et al. 2016). Accordingly, our RNA-seq data revealed a significant downregulation of these genes in the *max2* mutant when compared to the WT (Fig. 3A). However, the expression level remained unchanged upon treatment with *rac*-GR24. qRT-PCR analysis of these genes in the *d14*, *kai2, d14;kai2,* and *max2* mutants indicated that the expression levels of *CHS* and *FLS1* were significantly reduced in the roots of all tested mutants (Fig. 3B). In contrast, *PAL1* expression was not significantly different from Col-0, which is in agreement with lower reduction detected in the RNA-seq data than that obtained for the other two genes (Fig. 3A, B). To conclude, the transcript levels of flavonoids-related genes, *CHS* and *FLS1,* is controlled by both D14 and KAI2. In contrast, *PAL1* that is involved in the phenylpropanoid pathway upstream of *CHS* and *FLS1*, seems not to be influenced by neither SL nor KAR/KL signaling.

MYB12 controls the flavonol accumulation in response to rac-*GR24 treatment*

Flavonol-related gene expression in the root is coordinated by three MYB transcription factors, *MYB11*, *MYB12,* and *MYB111* (Stracke et al. 2007). Interestingly, our RNA-seq data revealed a significantly lower basal expression level of the *MYB12,* but not of the *MYB11* or *MYB111*, transcription factor, in the *max2* than in the WT roots (Fig. 3A). The *MYB12* expression in SL and KAR signaling mutants analyzed by qRT-PCR was not significantly different from that of WT roots, although a slight downregulation was detected in *max2* roots (Fig. 3B). Nevertheless, qRT-PCR and histochemical analysis of *MYB12*-promoter GUS reporter lines revealed that the *MYB12* expression was induced by *rac*-GR24 in the WT roots (Fig. 3C, D). The increased *MYB12* expression after *rac*-GR24 treatment in the root was mostly visible in the elongation zone (Fig. 3D).

Next, we analyzed whether the three MYB transcription factors are required to coordinate the flavonol biosynthesis triggered by the *rac*-GR24 treatment. To this end, a high-performance thin-layer chromatography (HPTLC) was carried out on methanol extracts from the WT and the *myb11,myb111,myb12* triple mutant followed by DPBA staining (Fig. 4A). After 5 days of growth on medium containing 1 µM *rac*-GR24, the quercetin derivative levels, visible as orange fluorescence, had increased in the WT plants, but not in the triple mutant, suggesting that at least one of these transcription factors controls the *rac*-GR24–induced production of this flavonol in the root. To find out which transcription factor is responsible for this phenotype, we repeated the experiment with double and single mutants (Fig. 4B). The *rac*-GR24 treatment did not induce levels of quercetin derivatives in the roots of *myb12* mutants, whereas the response in the *myb11* and *myb111* mutants was similar to that of WT plants. No quercetin derivatives accumulated in the *myb12* seedlings and other mutants containing

the *myb12* allele grown under mock conditions (Fig. 4C). In contrast, the accumulation of kaempferol derivatives (blue fluorescence; Fig. 4) in response to *rac*-GR24 did not obviously differ. Together these data indicate that of the three MYB transcription factors at least MYB12 is required for the *rac*-GR24–dependent root flavonol response represented by accumulation of quercetin derivatives.

Next, the *CHS, FLS1,* and *PAL1* levels upon the *rac*-GR24 treatment were examined by qRT-PCR in the roots of the *myb12*. In contrast to WT plants, the expression of *CHS* and *FLS1* was not significantly induced in the mutant. Moreover, under mock conditions, their basal transcript levels were significantly lower in the *myb12* roots than those in the WT roots (Fig. 5A). On the contrary, the expression of the phenylpropanoid-related gene *PAL1* in the *myb12* and WT roots did not significantly differ and the induction upon the *rac*-GR24 treatment was comparable (Fig. 5A). Hence, these data imply that *MYB12* is exclusively necessary for the *rac*-GR24–induced flavonol response in the root by regulation of the flavonoid, but not the phenylpropanoid, biosynthesis genes.

As the *myb12* mutant shares the same aberrant flavonol response to the *rac*-GR24 treatment as *max2* (Walton et al. 2016), we investigated whether *MYB12* might be required for other root responses. However, the LRD of *myb12* seedlings did not differ from that of the WT upon *rac*-GR24 treatment (Fig. 5B), indicating that the *MYB12*-controlled flavonol response alone is not required for the LRD phenotype. Next, we examined whether another *rac*-GR24–related root phenotype, such as the modified root hair length, was affected in the *myb12* mutant. When grown under mock conditions, the root hairs of the *myb12* seedlings were significantly longer than those of the WT ($P \leq 0.001$, linear mixed model) and significantly less sensitive to the *rac*-GR24–induced elongation than Col-0 (52% and 87% increase, respectively; $P \leq 0.05$, linear mixed model; Fig. 5C). In conclusion, the *MYB12* action in the root accounts for the flavonol response toward *rac*-GR24 and influences the root hair length phenotype, but not the LRD.

The involvement of HY5 in rac-*GR24-induced flavonol accumulation, LRD reduction and root hair elongation*

The flavonol production has been described as one of the processes controlled by the key transcription factor *HY5* (Stracke et al. 2010b). In our RNA-seq analysis *HY5*, but also its homolog *HY5 HOMOLOG* (*HYH*) were downregulated in the *max2* mutant when compared to the WT (Fig. 6A). However, the expression of *HY5* in the *d14*, *kai2, d14;kai2*, and *max2* mutants analyzed by qRT-PCR did not significantly differ from the WT (Fig. 6B), possibly because the changes in RNA-seq dataset were too small. Nonetheless, we tested the *hy5-215* (*hy5*) mutant for various known *rac*-GR24 root responses. Whereas WT seedlings displayed a significant *(*$P \leq 0.001$, Poisson regression model) decrease of 25% in LRD upon treatment, this difference in the *hy5* mutant was not statistically significant (7,9%; Fig. 6C). Also, the root hair elongation of *hy5* seedlings was not affected by *rac*-GR24 (Supplementary Fig. S5). Subsequently, the flavonol production *in planta* in *hy5* and WT seedlings grown without or with *rac*-GR24 was visualized by DPBA staining. The flavonol accumulation was induced by the treatment with the SL analog in WT roots, but not in those of the *hy5* mutant (Fig. 6D). In addition, the overall flavonol content was lower in the *hy5* than that in WT plants under mock conditions. This reduced flavonol abundance could be attributed to a lower basal expression level of the *MYB12* gene in the *hy5* mutant when compared to WT and to the lack of the *rac*-GR24–induced increase in the *MYB12* transcript level in this mutant (Fig. 6E). Taken together, these results suggest that although *HY5* is not a direct target, it is involved in the

signaling cascade during the root responses to *rac*-GR24 that affects LRD, root hair length, and flavonol production, similarly to the phenotypes described for the *max2-1* mutant (Kapulnik et al. 2011b).

Possible role of TMO5/TMO5L1 as downstream transcription factors in the SL pathway in the root

Additionally, we searched our RNA-seq dataset for the transcription factors that might be involved in regulation of *rac*-GR24–mediated changes in the root architecture. To date, no candidate genes further downstream of the SMXL repressors have been identified that control these responses. Interestingly, we found the transcription factor *TARGET OF MONOPTEROS5* (*TMO5*)-*LIKE1* (*TMO5L1*) as the most significantly downregulated gene in the WT upon treatment with *rac*-GR24 (Supplementary Dataset S1). Furthermore, its homolog, TMO5, also had a reduced expression under the same conditions and both were upregulated in *max2* when compared to the WT in mock, hinting at a potential role for both as negative regulators of the *rac*-GR24 signaling (Fig. 7A). *TMO5* and *TMO5L1* are members of a clade of four homologous genes, *TMO5*, *TMO5L1*, *TMO5L2*, and *TMO5L3* (De Rybel et al. 2013). TMO5 and TMO5L1 form heterodimers with LONESOME HIGHWAY (LHW) to become transcriptionally active (Ohashi-Ito and Bergmann 2007; De Rybel et al. 2013) and control the initial process of the root vascular development and the root hair density in response to phosphate deficiency (Ohashi-Ito and Bergmann 2007; Wendrich et al. 2020).

As the reduction of the *TMO5L1* expression was the highest upon *rac*-GR24 treatment, the transcript level of this gene was investigated in the *d14*, *kai2, d14;kai2,* and *max2* mutants. It was significantly upregulated in the *d14*, *d14;kai2*, and *max2* mutants, but not in the *kai2* roots, indicating that the expression of this transcription factor is preferentially controlled by the *D14/MAX2* signaling cascade (Fig. 7B). In agreement, treatment with *rac*-GR24 in the WT reduced the *TMO5L1* expression after 6 h, confirming the RNA-seq results (Fig. 7C). Interestingly, downregulation of the *TMO5L1* expression in response to *rac*-GR24 was abolished in the *max2* mutant, indicating that this reduction requires an active SL/KAR signaling (Fig. 7C). Next, we examined the LRDs of the *tmo5, tmo5 like1,* and the *tmo5;tmo5 like1* double mutant in response to *rac*-GR24. Both single mutants showed hypersensitivity to *rac*-GR24, because the LRD reduction was significantly higher than that in the WT (*tmo5* 49% vs WT 40% and *tmo5 like1* 77% vs WT 64%; $P < 0.05$, Poisson regression model). Accordingly, the decrease in LRD in the *tmo5;tmo5 like1* double mutant was more significant than that of the WT (60% and 34%, respectively; $P < 0.001$, Poisson regression model) (Fig. 7D). Under mock conditions, all tested mutants were characterized by a LRD lower than that in the WT, with the most pronounced effect in the *tmo5;tmo5 like1* double mutant (Fig. 7D). In conclusion, we propose that the *TMO5* and *TMO5L1* transcription factors might be downstream components of the MAX2/D14 signaling pathway in the root, controlling the *rac*-GR24–regulated lateral root development.

Discussion

The remarkable ability of plants to react to their environment requires an extensive regulation in highly complex transcriptional networks. In reaction to various triggers, including light and hormones, or during specific developmental processes, such as programmed cell death, these networks activate downstream signals, but they can often also coexpress regulatory factors that allow the network to achieve its precise goal (Jiao et al. 2007;

Sun et al. 2010; Cubría-Radío and Nowack 2019). Here, we investigated the transcriptional responses activated by *rac*-GR24 in the roots of WT and *max2* plants.

The increased LRD in *max2* roots has been shown to depend on both KAI2 and D14 signaling (Villaécija-Aguilar et al. 2019), but how perception of exogenous *rac*-GR24 leads to a reduction in LRD is still not fully understood. Here we show that the *pft1* mutant is less sensitive to the *rac*-GR24 treatment in the roots. *PFT1* encodes a component of the Mediator complex, more specifically a part of the tail module, which is an important conveyor of information between gene-specific regulatory factors and the RNA polymerase II machinery (Samanta and Thakur 2015). Recently, SLs have been shown to activate downstream transcription for the regulation of shoot branching, leaf shape, and anthocyanin accumulation (Wang et al. 2020b). Here we demonstrate that transcriptional events are key also in the *rac*-GR24 impact on the LRD.

Analysis of the RNA-seq data revealed a number of transcriptional changes that occurred in the root upon *rac*-GR24 treatment, including an increase in the transcript levels of the negative regulators *SMAX1, SMXL2*, and *SMXL7*, starting 6 h post treatment. This induced expression might be a direct response to their *rac*-GR24–triggered degradation at the protein level that is visible at earlier time points (Soundappan et al. 2015; Struk et al. 2019; Van Overtveldt et al. 2019), suggesting that in this manner the SMXL proteins try to reestablish their repression of the SL and KAR/KL pathways. The gene expression induction has been previously detected for *SMXL2* and *SMXL6,7,8* but not *SMAX1* (Stanga et al. 2013; Wang et al. 2020b). The observed discrepancy in *SMAX1* expression with published data might be explained by the use of different tissues for the analysis. Additionally, the detection of reduced transcript levels of *SMAX1* and *SMXL2* in the *kai2,* but not *d14* mutant, concur with the pathway in which they function. In agreement, the *SMAX1* expression in 10-day-old seedlings has been shown to be induced by $GR24^{ent5DS}$, but not $GR24^{4DO}$, treatment (Wang et al. 2020a). This response depends on KAI2, further supporting our hypothesis that the *SMAX1* expression is solely controlled by KAI2. In contrast, the upregulation of *SMXL2* was detected after treatment with both $GR24^{ent5DS}$ and $GR24^{4DO}$ in a KAI2- and D14-dependent manner, respectively. This result does not fit with our observation that under mock conditions *SMXL2* seemed to be exclusively regulated by KAI2, but, under certain experimental conditions, such as treatment with a chemical SL analog, some interactions have been proposed to possibly be forced to occur creating a crosstalk between the SL and KAR pathways (Khosla et al. 2020). Although the relative expression of *SMXL7* did not significantly differ between the WT and all tested mutants, a slight reduction was discovered, in agreement with the small changes detected by RNA-seq. These results imply that in younger seedlings *SMAX1* and *SMXL2*, thus the KAI2 pathway, might play a more pronounced role than that of D14, as previously suggested (Villaécija-Aguilar et al. 2019). Overall, both RNA-seq and qRT-PCR data indicate that in the roots only minor transcriptional changes occur in the *SMAX1*, *SMXL2,* and *SMXL7* levels.

Beyond the negative regulators of the SL/KAR signaling, our dataset also contained genes involved in the phenylpropanoid pathway for flavonoid/flavonol production that were downregulated in the *max2* mutant, confirming our previously published proteome data (Walton et al. 2016). The expression of *CHS* and *FLS1* was reduced in all mutants, indicating that the endogenous root flavonol production at the seedling stage is controlled by both D14 and KAI2, in agreement with former data demonstrating that flavonol responses to exogenous *rac*-GR24 treatments are mediated by both receptors (Walton et al. 2016). Similarly, the anthocyanin accumulation seems to be regulated by both pathways as well (Wang at al. 2020b; Bursch et al. 2021).

Out of the three MYB transcription factors known to control flavonol biosynthesis, the *rac*-GR24–induced flavonol (possibly quercetin derivatives) accumulation, is regulated at least by *MYB12* that itself is induced by the SL analog in a *MAX2*-dependent manner. Promoter-GUS experiments demonstrated the *rac*-GR24–induced *MYB12* expression in the root elongation zone, i.e., the same cellular localization in which *proSMXL2:GUS* is induced upon *rac-GR24* treatment and the fluorescent SL analog yoshimulactone green is hydrolyzed, indicating that this zone might be an active site for SL/KAR perception (Tsuchiya et al. 2015). Accordingly, *MYB12* regulates the expression of genes specific for the flavonoid pathway (Stracke et al. 2010b), but not of genes acting upstream in the phenylpropanoid path, such as *PAL1*. Here we show that *rac*-GR24 induces also flavonoid/flavonol accumulation in the root by inducing biosynthesis genes, such as *CHS* and *FLS1* and that this process depends on both D14 and KAI2 as well as on the MYB12 transcription factor.

Flavonols have been reported to negatively regulate both LRD and root hair growth by affecting auxin transport and/or scavenging ROS (Lewis et al. 2011; Grunewald et al. 2012; Gayomba et al. 2016; Tan et al. 2019; Gayomba and Muday 2020; Chapman and Muday 2021). Like SLs, flavonols have been linked to auxin transport and signaling in the root as well (Kuhn et al. 2017; Tan et al. 2019; Grunewald et al. 2012). Indeed, an increased flavonol content in root has been negatively correlated with auxin levels in agreement with an enhanced competition for auxin upon SL treatment (Crawford et al. 2010; Jiang et al. 2016; Tan et al. 2019). Moreover, a localization shift of PIN-FORMED 2 from the basal to the apical side in *Arabidopsis* root tips has been described to depend on the presence of flavonols, clearly showing that these compounds can directly influence the auxin flow (Kuhn et al. 2017). Phenotypically, the *myb12* mutant remained sensitive to *rac*-GR24 in the LRD assay, implying that the MYB12-dependent flavonol accumulation alone does not account for this response. However, we cannot rule out that *MYB11* and *MYB111* might play a minor role and that only a complete lack of flavonols in the triple mutant would hamper the *rac*-GR24–triggered effect on the LRD.

Mutants with defects in genes encoding key enzymes of the flavonoid biosynthesis, such as *transparent testa 4* (*tt4*), are characterized by increased root hair formation (root hair density) (Gayomba and Muday, 2020). The *myb12* seedlings had significantly longer root hairs under mock conditions, possibly due to an increased auxin content, known to promote root hair development, as a consequence of decreased flavonol levels (Dindas et al., 2018; Tan et al., 2019). However, to verify whether, besides the root hair density, reduced flavonol levels regulate also the root hair length, this phenotype should be tested in *tt4* or other flavonol biosynthesis mutants that show no changes in the *MYB12* expression. Furthermore, the crosstalk between flavonols, auxin, and SL/KAR signaling regarding root hair development remains unclear and requires further investigation. Similarly, as in the case of the LRD, the role of *MYB11* and *MYB111* should be considered as well. As SLs, *rac*-GR24, and flavonoids are known to be involved in the communication with the rhizosphere organisms, the flavonoids observed here might perhaps mediate such functions, in addition to their role in root development (Abdel-Lateif et al. 2012; López-Ráez et al. 2017). Also the KAR/KL signaling has been proposed to shape the rhizomicrobiome composition by promoting the biosynthesis of flavonoids (Nasir et al. 2020).

The transcription factor HY5 has been linked to *rac*-GR24 and KAR/KL responses in the hypocotyl downstream of SMAX1 and SMXL2, such as control of the *CHS* expression and anthocyanin accumulation (Nelson et al. 2010; Waters and Smith 2013; Bursch et al. 2021), but also of the hypocotyl length (Tsuchiya et al. 2010; Bursch et al. 2021). *HY5* modulates light responses during seedling growth by regulating the light-dependent transcriptional networks (Koornneef et al. 1980; Osterlund et al. 2000; Cluis et al. 2004). Similarly to

the *max2* mutant, the *hy5* seedlings have an elongated hypocotyl and are less responsive to the *rac*-GR24– and KAR_2– induced hypocotyl growth inhibition (Tsuchiya et al. 2010; Bursch et al. 2021). *HY5* has also been shown to regulate the emergence of lateral roots in a shoot-derived auxin-dependent process, attributed to an inhibition of the lateral root emergence rather than to an effect on the lateral root priming or initiation (Cluis et al. 2004).

Here we have uncovered an additional role for HY5 in the control of the *rac*-GR24 effects in the root. *HY5* and its homolog *HYH* were detected as significantly downregulated in *max2* in comparison to WT roots under mock conditions, although this result could not be validated by the qRT-PCR analysis. HY5 has been previously reported to increase the flavonol content in the roots by transcriptional activation of several flavonoid biosynthesis genes (Sibout et al. 2006; Stracke et al. 2010b; Shin et al. 2013; Zhang et al. 2019). Here we show that HY5 is also essential for the *rac*-GR24–dependent flavonol readout and *MYB12* expression, just like MAX2, in agreement with previous studies suggesting that *MYB12* is under *HY5* control in the root (Stracke et al. 2010b). Furthermore, as in case of the hypocotyl phenotype, the *hy5* seedlings were insensitive to the *rac*-GR24 treatment in the LRD and root hair length assays. Thus, our findings indicate that the *rac*-GR24–triggered flavonol response and the *MYB12* expression depend on both *MAX2* and *HY5*. Although this pathway is not responsible for the root phenotypes in the mutants, other members of the *MYB12*-independent part of the *HY5*-triggered network could potentially be redundantly involved. The *hy5* insensitivity to *rac*-GR24 in both root and seedling phenotypes definitely provides a strong link to *max2*. Perhaps the observed similarities might be attributed to the altered auxin landscape in both mutants (Sassi et al. 2012).

Another candidate regulator of the transcriptional network of *rac*-GR24 that was identified in the root is *TMO5L1*. This transcription factor has previously been shown to control the cell divisions that underlie the establishment and indeterminate growth of the root vascular tissue by a direct induction of the cytokinin biosynthesis genes of the LONELY GUY (LOG) family, resulting in elevated cytokinin levels in the surrounding cells (De Rybel et al. 2013, 2014; Ohashi-Ito et al. 2014). In addition, the TMO5L1/LHW complex also regulates xylem differentiation and development in the root apical meristem in a negative feedback loop (Katayama et al. 2015; Vera-Sirera et al. 2015). Analysis of the positions of TMO5 and TMO5L1 in the receptor pathway revealed that they might act downstream of D14 rather than of KAI2. In agreement, both genes were not found to be differentially expressed in the *smxl1 smxl2* seedlings when compared to the wild-type in the recently published transcriptome (Bursch et al. 2021). The phenotypes of *tmo5*, *tmo5 like1*, and the double mutant were all hypersensitive to the *rac*-GR24 treatment, with a significantly larger reduction in LRD than that in WT plants. Thus, *TMO5* and *TMO5L1* might be negative regulators of the *rac*-GR24 signaling and their expression might be an early marker of the *rac*-GR24 response in the root. The next step will now be to unravel how MAX2 signaling causes the observed reduction in the *TMO5/TMLO5L1* transcript level and whether it occurs through transcriptional changes (e.g. by chromatin remodeling or binding of the transcription factor to the promoters) or through posttranscriptional control of the mRNA stability. A crosstalk between SL/KAR and cytokinin during lateral root formation could also account for the phenotypes of *tmo5;tmo5 like1*, because the cytokinin module ARABIDOPSIS HISTIDINE KINASE3 (AHK3)/ARABIDOPSIS RESPONSE REGULATOR1 (ARR1)/ARR12 interacted with the *rac*-GR24–dependent reduction in lateral root development (Jiang et al. 2016).

Recently, the TMO5/LHW heterodimer has been demonstrated to increase root hair length and density under limited phosphate conditions by triggering the cytokinin biosynthesis in vascular cells, whereas TMO5L1 seemed to be redundantly required for this response (Wendrich et al. 2020). This finding might suggest yet another link between TMO5/TMO5L1 and MAX2 signaling. Under phosphate-deprived conditions, the exogenous *rac*-GR24 is known to promote root hair density in WT and, accordingly, the root hair density is strongly reduced in the *max2* mutant (Kapulnik et al. 2011b). Hence, it would be interesting to investigate whether TMO5/TMO5L1 is involved in *rac*-GR24–induced root hair elongation and density, however some inconsistencies still remain to be considered. Although the control of the root hair phenotypes has previously been attributed to SL signaling, recently this response has been shown to be mediated by the KAI2 pathway (Villaécija-Aguilar et al. 2019), whereas our qRT-PCR data suggested that *TMO5L1* is involved in the D14 signaling. Secondly, TMO5 and TMO5L1 play a positive role in root hair development under limited phosphate conditions, but we here show that they negatively regulate *rac*-GR24–induced reduction in LRD. This apparent contraction is definitely the basis for further investigation.

In conclusion, we provide insights into the transcriptional responses triggered by *rac*-GR24 in the root. Transcriptional changes, albeit small, are important for the phenotypic effects of *rac*-GR24 on the root and can position the Mediator complex, *HY5, MYB12*, and *TMO5L1* as novel downstream signaling components.

Materials and methods

Plant material

Seeds of *Arabidopsis thaliana* (L.) Heyhn. (accession Columbia-0) were surface sterilized with consecutive treatments of 70% (v/v) ethanol with 0.05% (w/v) sodium dodecyl sulfate (SDS), and then washed with 95% (v/v) ethanol. The *max2-1* (Stirnberg et al. 2002), *kai2/htl-3*, *d14;kai2/htl-3* (Toh et al. 2014), *d14* (Waters et al. 2012), *hy5-215* (Oyama et al. 1997), *pft1-3* and *pft1-2* (Kidd et al. 2009), *myb11*, *myb12* and *myb111* (Stracke et al. 2007), *tmo5* and *tmo5like1* (De Rybel et al. 2013) mutants were in the Col-0 background and had been described previously. For material destined for RNA preparation, seeds were sown on nylon meshes (Ø 20 µm; Nytal® Prosep, Zaventem, Belgium) placed on half-strength Murashige and Skoog (½MS) medium containing 1% (w/v) sucrose. Seeds were stratified for 2 days at 4°C, whereafter they were grown for 5 days under continuous light conditions at 21°C, before transfer to mock (0.01% [v/v] acetone) or 1 µM *rac*-GR24–containing medium.

RNA extraction and quantitative (q)RT-PCR

Approximately 30 roots of 5-day-old plants were harvested for each biological repeat and snap-frozen in liquid nitrogen. RNA was extracted and purified with the ReliaPrep^{TM} RNA Tissue Miniprep System (Promega) according to the manufacturer's instructions. The iScript cDNA synthesis kit (Bio-Rad) was used to reverse transcribe RNA. All primers are listed in Supplementary Table S3. SYBR Green detection was used during the qRT-PCR runs on a Light Cycler 480 (Roche). Reactions were done in triplicate in a 384-multiwell plate, in a total volume of 5 µl and a cDNA fraction of 10%. Cycle threshold values were obtained and analyzed with the 2-

ΔΔCT method (Livak and Schmittgen 2001). The values from three to four biological repeats and three technical repeats were normalized against those of *ACTIN2* (*ACT2*, AT3G18780), *TUBULIN BETA CHAIN 2* (*TUB2*, AT5G62690), and PROTEIN PHOSPHATASE 2A SUBUNIT A3 (*PP2AA3*, AT1G13320).

RNA-seq analysis

Approximately 100 seedlings, grown as mentioned above, were used for each treatment and the experiment was repeated three times. RNA-seq was done after RNA quality control and in-house library preparation for mRNA enrichment. The samples were run on an Illumina HiSeq 2000 platform with a paired-end sequencing mode and a read length of 50 base pairs. The raw data files contained 15-18 million reads per sample. First, these data files were quality checked and filtered by FastQ manipulation that removed all reads for which more than 25% of the bases in the sequence had a quality score below the Q20 threshold (1% of total reads). Next, the 3'-end were trimmed with the FastQ Qual trimmer that removed all ends with a quality score below Q10. Lastly, reads were paired forward and reverse and mapped on the *Arabidopsis* genome by means of the annotated genome of The Arabidopsis Information Resource (TAIR10). Each of the reads were assigned to a specific gene, resulting in a table with raw counts per gene. The raw data and following differential expression analysis were normalized with EdgeR, a plugin for R software, and with the default settings. After statistical analysis, the fold-change (FC) threshold was set between 1.2 and 0.83 and False Discovery Rate (FDR) below 0.05 to select potentially biologically relevant genes.

DPBA staining and HPTLC

DPBA staining and HPTLC were done as previously described (Walton et al. 2016). After methanol extraction from the root tissue, samples were dried with a concentrator 5301 (Eppendorf), and resuspended in 20 µl of an 80% (v/v) methanol solution. Of the mixture, 2 µl was spotted onto a 20 cm×10 cm silica-60 HPTLC glass plate (Merck) and placed in a glass tank with a paper wick of 18 cm by 9 cm (Whatman) and a mobile polar phase consisting of ethyl acetate, dichloromethane, acetic acid, formic acid, and water in a 100:25:10:10:11 ratio. After addition of the mobile phase, the glass tank was sealed with silicon grease and plates were run for 25 min. Plates were stained by spraying a methanol solution containing 1% (v/v) diphenylboric acid 2-aminoethylester (DPBA). Plates were placed into an HB-1000 Hybridizer (Thermo Fisher Scientific) at 100°C for 10 min, whereafter the plates were sprayed with a 5% (w/v) PEG-3350 (Merck) solution in methanol (100%) to stabilize the DPBA compound. Plates were observed after UV excitation at 350 nm.

Root phenotypes

The roots of 9-day-old seedlings were counted under a S4E light microscope (Leica Microsystems), and the main root length was measured with the ImageJ software. The root hair length of 5-day-old seedlings were measured with the ImageJ software in a 1-mm segment of the primary root, in which hairs were fully elongated, approximately at the same distance from the root tip (Fernandez et al. 2013).

GUS staining

The *proSMXL2:GUS* and *proSMXL7:GUS* reporter lines were constructed by cloning a 3-kb promoter region upstream of the ATG start codon and transforming the construct in Col-0. Homozygous lines of the two *proSMXL:GUS* lines and the *proMYB12::GUS* (Stracke et al. 2007) were grown for 7 days on ½MS media with 1% (w/v) sucrose and in the presence of 1 µM *rac*-GR24 or 0.01% (v/v) acetone (mock). Complete seedlings were stained in multiwell plates as described (Jefferson et al. 1987). Each step was done for 30 min, except for the last step, incubation in assay solution (2.5 mM 5-bromo-4-chloro-3-indolyl-β-D-glucuronic acid (Thermo Scientific) in ferricyanide solution, that lasted according to the gene expression: 2 h for *proSMXL2:GUS* and overnight for *proSMXL7:GUS* and *proMYB12:GUS*. Samples were mounted in 50% (v/v) glycerol and were observed by differential interference contrast (DIC) microscopy (DMLB; Olympus BX51) (Arnison et al. 2004).

Supplementary data

Supplementary data are available at PCP online.

Funding

This work was supported by the European Cooperation on Science and Technology (COST action FA1206), the Research Foundation-Flanders (Strategic Basic Research fellowship to L.B. and postdoctoral fellowship to E.S.), the "Bijzonder Onderzoeksfonds" of the Ghent University (predoctoral fellowship for C.M.), the VIB International PhD program (fellowship to A.W.), and the China Science Council (fellowship to L.J.).

Acknowledgements

We thank Ralf Stracke (Bielefeld University, Bielefeld, Germany) for providing the *myb* mutants and our colleagues Bert De Rybel for the *tmo5/tmo5l1* double mutant, Boris Parizot for tips on the RNA-seq analysis, Veronique Storme for statistical help on both the RNA-seq and lateral root density, and Martine De Cock for help in preparing the manuscript.

Data Availability Statement

The data underlying this article are available in the article and in its online supplementary material.

Disclosures

The authors have no conflicts of interest to declare.

References

Abdel-Lateif, K., Bogusz, D. and Hocher, V. (2012) The role of flavonoids in the establishment of plant roots endosymbioses with arbuscular mycorrhiza fungi, rhizobia and *Frankia* bacteria. *Plant Signal. Behav*. 7: 636-641.

Akiyama, K., Matsuzaki, K.-i. and Hayashi, H. (2005) Plant sesquiterpenes induce hyphal branching in arbuscular mycorrhizal fungi. *Nature* 435, 824-827.

Arnison, M.R., Larkin, K.G., Sheppard, C.J.R., Smith, N.I. and Cogswell, C.J. (2004) Linear phase imaging using differential interference contrast microscopy. *J. Microsc*. 214, 7-12.

Baster, P. (2014) Regulatory mechanisms for vacuolar trafficking of PIN auxin transporters. PhD dissertation. Ghent University, Ghent, Belgium.

Bennett, T., Liang, Y., Seale, M., Ward, S., Müller, D. and Leyser, O. (2016) Strigolactone regulates shoot development through a core signalling pathway. *Biol. Open* 5: 1806-1820.

Bergmann, C., Wegmann, K., Frischmuth, K., Samson, E., Kranz, A., Weigelt, D., et al. (1993) Stimulation of *Orobanche crenata* seed germination by (+)-strigol and structural analogues dependence on constitution and configuration of the germination stimulants. *J. Plant Physiol*. 142, 338–342.

Bhatia, C., Gaddam, S.R., Pandey, A. and Trivedi, P.K. (2021) COP1 mediates light-dependent regulation of flavonol biosynthesis through HY5 in Arabidopsis. *Plant Sci.* 303: 110760.

Bursch, K., Niemann, E.T., Nelson, D.C. and Johansson, H. (2021) Karrikins control seedling photomorphogenesis and anthocyanin biosynthesis through a HY5-BBX transcriptional module. *Plant J.*: in press (doi: 10.1111/tpj.15383).

Chapman, J.M. and Muday, G.K. (2021) Flavonols modulate lateral root emergence by scavenging reactive oxygen species in *Arabidopsis thaliana*. *J. Biol. Chem.* 296: 100222.

Cluis, C.P., Mouchel, C.F. and Hardtke, C.S. (2004) The *Arabidopsis* transcription factor HY5 integrates light and hormone signaling pathways. *Plant J*. 38: 332-347.

Conn, C.E. and Nelson, D.C. (2016) Evidence that KARRIKIN-INSENSITIVE2 (KAI2) receptors may perceive an unknown signal that is not karrikin or strigolactone. *Front. Plant Sci.* 6: 1219.

Cook, C.E., Whichard, L.P., Turner, B., Wall, M.E. and Egley, G.H. (1966) Germination of witchweed (*Striga lutea* Lour.): isolation and properties of a potent stimulant. *Science* 154: 1189-1190.

Crawford, S., Shinohara, N., Sieberer, T., Williamson, L., George, G., Hepworth, J., et al. (2010) Strigolactones enhance competition between shoot branches by dampening auxin transport. *Development* 137: 2905-2913.

Cubría-Radío, M. and Nowack, M.K. (2019) Transcriptional networks orchestrating programmed cell death during plant development. *Curr. Topics Dev. Biol*. 131: 161–184.

De Cuyper, C., Struk, S., Braem, L., Gevaert, K, De Jaeger, G. and Goormachtig, S. (2017) Strigolactones, karrikins and beyond. *Plant Cell Environ*. 40: 1691-1703.

De Rybel, B., Abidi, M., Breda, A.S., Wendrich, J.R., Smit, M.E., Novák, O., et al. (2014) Integration of growth and patterning during vascular tissue formation in *Arabidopsis*. *Science* 345, 1255215.

De Rybel, B., Möller, B., Yoshida, S., Grabowicz, Barbier de Reuille, P., Boeren, S., Smith, R.S., Borst, J.W.,and Weijers, D. (2013) A bHLH complex controls embryonic vascular tissue establishment and indeterminate growth in *Arabidopsis*. *Dev. Cell* 24: 426-437.

Dindas, J., Scherzer, S., Roelfsema, M.R.G., von Meyer, K., Müller, H.M., Al-Rasheid, K.A.S., et al. (2018) AUX1-mediated root hair auxin influx governs $SCF^{TIR1/AFB}$-type Ca^{2+} signaling. *Nat. Commun.* 9: 1174.

Fernandez, A., Drozdzecki, A., Hoogewijs, K., Nguyen, A., Beeckman, T., Madder, A., et al. (2013) Transcriptional and functional classification of the GOLVEN/ROOT GROWTH FACTOR/CLE-like signaling peptides reveals their role in lateral root and hair formation. *Plant Physiol.* 161: 954-970.

Gayomba, S.R. and Muday, G.K. (2020) Flavonols regulate root hair development by modulating accumulation of reactive oxygen species in the root epidermis. *Development* 147: dev185819.

Gayomba, S.R., Watkins, J.M. and Muday, G.K. (2017) Flavonols regulate plant growth and development through regulation of auxin transport and cellular redox status. In *Recent Advances in Polyphenol Research*. Edited by Yoshida, K., Cheynier, V. and Quideau, S. pp. 143-170. John Wiley & Sons, Chichester (U.K.).

Grunewald, W., De Smet, I., Lewis, D.R., Löfke, C., Jansen, L., Goeminne, G., et al. (2012) Transcription factor WRKY23 assists auxin distribution patterns during *Arabidopsis* root development through local control on flavonol biosynthesis. *Proc. Natl. Acad. Sci. USA* 109: 1554-1559.

Guo, Y., Zheng, Z., La Clair, J.J., Chory, J. and Noel, J.P. (2013) Smoke-derived karrikin perception by the α/β-hydrolase KAI2 from *Arabidopsis*. *Proc. NatL. Acad. Sci. USA* 110: 8284-8289.

Jefferson, R.A., Kavanagh, T.A. and Bevan, M.W. (1987) GUS fusions: *β*-glucuronidase as a sensitive and versatile gene fusion marker in higher plants. *EMBO J*. 6: 3901-3907.

Jiang, L., Matthys, C., Marquez-Garcia, B., De Cuyper, C., Smet, L., De Keyser, A., et al. (2016) Strigolactones spatially influence lateral root development through the cytokinin signaling network. *J. Exp. Bot.* 67: 379-389.

Jiao, Y., Lau, O.S. and Deng, X.W. (2007) Light-regulated transcriptional networks in higher plants. *Nat. Rev. Genet*. 8: 217-230.

Kagey, M.H., Newman, J.J., Bilodeau, S., Zhan, Y., Orlando, D.A., van Berkum, N.L., et al. (2010) Mediator and cohesin connect gene expression and chromatin architecture. *Nature* 467: 430-435.

Kapulnik, Y. and Koltai, H. (2014) Strigolactone involvement in root development, response to abiotic stress, and interactions with the biotic soil environment. *Plant Physiol*. 166: 560-569.

Kapulnik, Y., Delaux, P.-M., Resnick, N., Mayzlish-Gati, E., Wininger, S., Bhattacharya, C., et al. (2011a) Strigolactones affect lateral root formation and root-hair elongation in *Arabidopsis*. *Planta* 233: 209-216.

Kapulnik, Y., Resnick, N., Mayzlish-Gati, E., Kaplan, Y., Wininger, S., Hershenhorn, J. and Koltai, H. (2011b) Strigolactones interact with ethylene and auxin in regulating root-hair elongation in *Arabidopsis*. *J. Exp. Bot*. 62: 2915-2924.

Katayama, H., Iwamoto, K., Kariya, Y., Asakawa, T., Kan, T., Fukuda, H. and Ohashi-Ito, K. (2015) A negative feedback loop controlling bHLH complexes is involved in vascular cell division and differentiation in the root apical meristem. *Curr. Biol*. 25: 3144–3150.

Khosla, A., Morffy, N., Li, Q., Faure, L., Chang, S.H., Yao, J., et al. (2020) Structure–function analysis of SMAX1 reveals domains that mediate its karrikin-induced proteolysis and interaction with the receptor KAI2. *Plant Cell* 32: 2639-2659.

Kidd, B.N., Edgar, C.I., Kumar, K.K., Aitken, E.A., Schenk, P.M., Manners, J.M., et al. (2009) The Mediator complex subunit PFT1 is a key regulator of jasmonate-dependent defense in *Arabidopsis*. *Plant Cell* 21: 2237-2252.

Kobae, Y., Kameoka, H., Sugimura, Y., Saito, K., Ohtomo, R., Fujiwara, T. and Kyozuka, J. (2018) Strigolactone biosynthesis genes of rice are required for the punctual entry of arbuscular mycorrhizal fungi into the roots. *Plant Cell Physiol*. 59: 544–553.

Koornneef, M., Rolff, E. and Spruit, C.J.P. (1980) Genetic control of light-inhibited hypocotyl elongation in *Arabidopsis thaliana* (L.) Heynh. *Z. Pflanzenphysiol*. 100: 147-160.

Kuhn, B.M., Nodzyński, T., Errafi, S., Bucher, R., Gupta, S., Aryal, B., et al. (2017) Flavonol-induced changes in PIN2 polarity and auxin transport in the *Arabidopsis thaliana rol1-2* mutant require phosphatase activity. *Sci. Rep.* 7: 41906.

Lewis, D.R., Ramirez, M.V., Miller, N.D., Vallabhaneni, P., Ray, W.K., Helm, R.F., et al. (2011) Auxin and ethylene induce flavonol accumulation through distinct transcriptional networks. *Plant Physiol.* 156: 144-164.

Lex, A., Gehlenborg, N., Strobelt, H., Vuillemot, R. and Pfister, H. (2014) UpSet: Visualization of intersecting sets. *IEEE Trans. Vis. Comput. Graph.* 20: 1983-1992.

Liang, Y., Ward, S., Li, P., Bennett, T. and Leyser, O. (2016) SMAX1-LIKE7 signals from the nucleus to regulate shoot development in Arabidopsis via partially EAR motif-independent mechanisms. *Plant Cell* 28: 1581-1601.

Livak, K.J. and Schmittgen, T.D. (2001) Analysis of relative gene expression data using real-time quantitative PCR and the $2^{-\Delta\Delta C_T}$ method. *Methods* 25: 402-408.

López-Ráez, J.A., Shirasu, K. and Foo, E. (2017) Strigolactones in plant interactions with beneficial and detrimental organisms: the yin and yang. *Trends Plant Sci*. 22: 527–537.

Mehrtens, F., Kranz, H., Bednarek, P. and Weisshaar, B. (2005) The Arabidopsis transcription factor MYB12 is a flavonol-specific regulator of phenylpropanoid biosynthesis. *Plant Physiol.* 138: 1083-1096.

Nasir, F., Li, W., Tran, L.P. and Tian, C. (2020) Does karrikin signaling shape the rhizomicrobiome via the strigolactone biosynthetic pathway? *Trends Plant Sci.* 25: 1184-1187.

Nelson, D.C., Flematti, G.R., Riseborough, J.-A., Ghisalberti, E.L., Dixon, K.W. and Smith, S.M. (2010) Karrikins enhance light responses during germination and seedling development in *Arabidopsis thaliana*. *Proc. NatL. Acad. Sci. USA* 107: 7095-7100.

Nelson, D.C., Scaffidi, A., Dun, E.A., Waters, M.T., Flematti, G.R., Dixon, K.W., et al. (2011) F-box protein MAX2 has dual roles in karrikin and strigolactone signaling in *Arabidopsis thaliana*. *Proc. NatL. Acad. Sci. USA* 108: 8897-8902.

Ohashi-Ito, K. and Bergmann, D.C. (2007) Regulation of the *Arabidopsis* root vascular initial population by *LONESOME HIGHWAY*. *Development* 134: 2959-2968.

Ohashi-Ito, K., Saegusa, M., Iwamoto, K., Oda, Y., Katayama, H., Kojima, M., et al. (2014) A bHLH complex activates vascular cell division via cytokinin action in root apical meristem. *Curr. Biol*. 24: 2053–2058.

Osterlund, M.T., Wei, N. and Deng, X.W. (2000) The roles of photoreceptor systems and the COP1-targeted destabilization of HY5 in light control of Arabidopsis seedling development. *Plant Physiol*. 124: 1520-1524.

Oyama, T., Shimura, Y. and Okada, K. (1997) The *Arabidopsis HY5* gene encodes a bZIP protein that regulates stimulus-induced development of root and hypocotyl. *Genes Dev*. 11: 2983-2995.

Ruyter-Spira, C., Kohlen, W., Charnikhova, T., van Zeijl, A., van Bezouwen, L., de Ruijter, N., et al. (2011) Physiological effects of the synthetic strigolactone analog GR24 on root system architecture in Arabidopsis: another belowground role for strigolactones? *Plant Physiol*. 155: 721-734.

Samanta, S. and Thakur, J.K. (2015) Importance of Mediator complex in the regulation and integration of diverse signaling pathways in plants. *Front. Plant Sci.* 6: 757.

Sassi, M., Lu, Y., Zhang, Y., Wang, J., Dhonukshe, P., Blilou, I., et al. (2012) COP1 mediates the coordination of root and shoot growth by light through modulation of PIN1- and PIN2-dependent auxin transport in *Arabidopsis*. *Development* 139: 3402-3412.

Scaffidi, A., Waters, M.T., Sun, Y.K., Skelton, B.W., Dixon, K.W., Ghisalberti, E.L., et al. (2014) Strigolactone Hormones and their stereoisomers signal through two related receptor proteins to induce different physiological responses in Arabidopsis. *Plant Physiol.* 165: 1221-1232.

Shin, D.H., Choi, M., Kim, K., Bang, G., Cho, M., Choi, S.-B., et al. (2013) HY5 regulates anthocyanin biosynthesis by inducing the transcriptional activation of the MYB75/PAP1 transcription factor in *Arabidopsis*. *FEBS Lett.* 587: 1543-1547.

Shinohara, N., Taylor, C. and Leyser, O. (2013) Strigolactone can promote or inhibit shoot branching by triggering rapid depletion of the auxin efflux protein PIN1 from the plasma membrane. *PLoS Biol*. 11: e1001474.

Sibout, R., Sukumar, P., Hettiarachchi, C., Holm, M., Muday, G.K. and Hardtke, C.S. (2006) Opposite root growth phenotypes of *hy5* versus *hy5 hyh* mutants correlate with increased constitutive auxin signaling. *PLoS Genet.* 2: e202.

Silva-Navas, J., Moreno-Risueno, M.A., Manzano, C., Téllez-Robledo, B., Navarro-Neila, S., Carrasco, V., et al. (2016) Flavonols mediate root phototropism and growth through regulation of proliferation-to-differentiation transition. *Plant Cell* 28: 1372-1387.

Soundappan, I., Bennett, T., Morffy, N., Liang, Y., Stanga, J.P., Abbas, A., et al. (2015) SMAX1-LIKE/D53 family members enable distinct MAX2-dependent responses to strigolactones and karrikins in Arabidopsis. *Plant Cell* 27: 3143-3159.

Stanga, J.P., Morffy, N. and Nelson, D.C. (2016) Functional redundancy in the control of seedling growth by the karrikin signaling pathway. *Planta* 243: 1397-1406.

Stanga, J.P., Smith, S.M., Briggs, W.R. and Nelson, D.C. (2013) *SUPPRESSOR OF MORE AXILLARY GROWTH2 1* controls seed germination and seedling development in Arabidopsis. *Plant Physiol*. 163: 318-330.

Stirnberg, P., van de Sande, K. and Leyser, H.M.O. (2002) *MAX1* and *MAX2* control shoot lateral branching in *Arabidopsis*. *Development* 129: 1131-1141.

Stracke, R., Ishihara, H., Huep, G., Barsch, A., Mehrtens, F., Niehaus, K., et al. (2007) Differential regulation of closely related R2R3-MYB transcription factors controls flavonol accumulation in different parts of the *Arabidopsis thaliana* seedling. *Plant J.* 50: 660-677.

Stracke, R., Jahns, O., Keck, M., Tohge, T., Niehaus, K., Fernie, A.R., et al. (2010a) Analysis of PRODUCTION OF FLAVONOL GLYCOSIDES-dependent flavonol glycoside accumulation in *Arabidopsis thaliana* plants reveals MYB11-, MYB12- and MYB111-independent flavonol glycoside accumulation. *New Phytol.* 188: 985-1000.

Stracke, R., Favory, J.-J., Gruber, H., Bartelniewoehner, L., Bartels, S., Binkert, M., et al. (2010b) The *Arabidopsis* bZIP transcription factor HY5 regulates expression of the *PFG1/MYB12* gene in response to light and ultraviolet-B radiation. *Plant Cell Environ*. 33: 88-103.

Struk, S., Jacobs, A., Sánchez Martín-Fontecha, E., Gevaert, K., Cubas, P. and Goormachtig, S**.** (2019) Exploring the protein-protein interaction landscape in plants. *Plant Cell Environ.* 42: 387-409.

Sun, Y., Fan, X.-Y., Cao, D.-M., Tang, W., He, K., Zhu, J.-Y., et al. (2010) Integration of brassinosteroid signal transduction with the transcription network for plant growth regulation in *Arabidopsis*. *Dev. Cell* 19: 765-777.

Swarbreck, S.M., Guerringue, Y., Matthus, E., Jamieson, F.J.C. and Davies, J.M. (2019) Impairment in karrikin but not strigolactone sensing enhances root skewing in *Arabidopsis thaliana*. *Plant J.* 98: 607-621.

Swarbreck, S.M., Mohammad-Sidik, A. and Davies, J.M. (2020) Common components of the strigolactone and karrikin signaling pathways suppress root branching in Arabidopsis. *Plant Physiol.* 184: 18-22.

Tan, H., Man, C., Xie, Y., Yan, J., Chu, J. and Huang, J. (2019) A crucial role of GA-regulated flavonol biosynthesis in root growth of *Arabidopsis*. *Mol. Plant* 12: 521-537.

Taylor, L.P. and Grotewold, E. (2005) Flavonoids as developmental regulators. *Curr. Opin. Plant Biol.* 8: 317-323.

Toh, S., Holbrook-Smith, D., Stokes, M.E., Tsuchiya, Y. and McCourt, P. (2014) Detection of parasitic plant suicide germination compounds using a high-throughput *Arabidopsis* HTL/KAI2 strigolactone perception system. *Chem. Biol.* 21: 988-998 [Erratum *Chem. Biol.* 21: 1253].

Tsuchiya, Y., Vidaurre, D., Toh, S., Hanada, A., Nambara, E., Kamiya, Y., et al. (2010) A small-molecule screen identifies new functions for the plant hormone strigolactone. *Nat. Chem. Biol*. 6: 741-749.

Tsuchiya, Y., Yoshimura, M., Sato, Y., Kuwata, K., Toh, S., Holbrook-Smith, D., et al. (2015) Probing strigolactone receptors in *Striga hermonthica* with fluorescence. *Science* 349: 864-868.

Van Overtveldt, M., Braem, L., Struk, S., Kaczmarek, A.M., Boyer, F.D., Van Deun, R., et al. (2019) Design and visualization of second-generation cyanoisoindole-based fluorescent strigolactone analogs. *Plant J.* 98: 165-180.

Vera-Sirera, F., De Rybel, B., Úrbez, C., Kouklas, E., Pesquera, M., Álvarez-Mahecha, J.C., et al. (2015) A bHLH-based feedback loop restricts vascular cell proliferation in plants. *Dev. Cell* 35, 432–443.

Villaécija-Aguilar, J.A., Hamon-Josse, M., Carbonnel, S., Kretschmar, A., Schmidt, C., Dawid, C., et al. (2019) SMAX1/SMXL2 regulate root and root hair development downstream of KAI2-mediated signalling in Arabidopsis. *PLoS Genet.* 15: e1008327.

Walton, A., Stes, E., Goeminne, G., Braem, L.,Vuylsteke, M., Matthys, C., et al. (2016) The response of the root proteome to the synthetic strigolactone GR24 in *Arabidopsis***.** *Mol. Cell. Proteomics* 15: 2744-2755.

Wang, L., Wang, B., Jiang, L., Liu, X., Li, X., Lu, Z., et al. (2015) Strigolactone signaling in Arabidopsis regulates shoot development by targeting D53-like SMXL repressor proteins for ubiquitination and degradation. *Plant Cell* 27: 3128-3142.

Wang, L., Wang, B., Yu, H., Guo, H., Lin, T., Kou, L., et al. (2020b) Transcriptional regulation of strigolactone signalling in *Arabidopsis*. *Nature* 583: 277-281.

Wang, L., Xu, Q., Yu, H., Ma, H., Li, X., Yang, J., et al. (2020a) Strigolactone and karrikin signaling pathways elicit ubiquitination and proteolysis of SMXL2 to regulate hypocotyl elongation in Arabidopsis. *Plant Cell* 32: 2251-2270.

Waters, M.T. and Smith, S.M. (2013) KAI2- and MAX2-mediated responses to karrikins and strigolactones are largely independent of HY5 in Arabidopsis seedlings. *Mol. Plant* 6: 63-75.

Waters, M.T., Nelson, D.C., Scaffidi, A., Flematti, G.R., Sun, Y.K., Dixon, K.W. and Smith, S.M. (2012) Specialisation within the DWARF14 protein family confers distinct responses to karrikins and strigolactones in *Arabidopsis*. *Development* 139: 1285-1295.

Wendrich, J.R., Yang, B., Vandamme, N., Verstaen, K., Smet, W., Van de Velde, C., et al. (2020) Vascular transcription factors guide plant epidermal responses to limiting phosphate conditions. *Science* 370.

Zhang, J., Mazur, E., Balla, J., Gallei, M., Kalousek, P., Medveďová, Z., et al. (2020) Strigolactones inhibit auxin feedback on PIN-dependent auxin transport canalization. *Nat. Commun.* 11: 3508.

Zhang, X., He, Y., Li, L., Liu, H. and Hong, G. (2021) Involvement of the R2R3-MYB transcription factor MYB21 and its homologs in regulating flavonol accumulation in Arabidopsis stamen. *J. Exp. Bot.* 72: 4319-4332.

Zhang, Y., Wang, C., Xu, H., Shi, X., Zhen, W., Hu, Z., et al. (2019) HY5 contributes to light-regulated root system architecture under a root-covered culture system. *Front. Plant Sci.* 10: 1490.

Figure Legends

Fig. 1. UpSet plot representation of overlaps of differentially expressed genes.
The numbers and overlaps of differentially expressed genes (Supplementary Datasets S1-S3) were determined and are shown as UpSet plot (Lex et al., 2014). The vertical bar chart gives the numbers of each genotype and condition, whereas the number of unique and overlapping genes is represented by horizontal bars, with the dot matrix indicating the respective overlaps by connected circles.

Fig. 2. Expression analysis of the *SMAX1, SMXL2*, and *SMXL7* genes.
(A) Table containing the AGI code, False Discovery Rate (FDR), and Fold Change (FC) for the genes from the Supplementary Datasets S1 and S2, color-coded for upregulation (red) or downregulation (blue). (B, C) Relative transcriptional levels of *SMAX1, SMXL2*, and *SMXL7* in the roots of Col-0 either treated under mock conditions or the with 1 µM *rac*-GR24 at different time points (B) and in Col-0*, d14, kai2*, *d14;kai2,* and *max2* mutants without any treatment (C). Transcript levels were measured in root tissues of 5-day-old seedlings by qRT-PCR and normalized to *ACT2*, *TUB2,* and *PP2AA3*. Error bars represent the standard error (SE), based on four independent biological repeats. (B) ANOVA mixed model with post hoc Tukey test ($P < 0.05$) comparing the expression levels of the *rac*-GR24–treated plants to the mock-treated ones at the same time point or (C) one-way ANOVA with post hoc Dunnett test ($P < 0.05$) comparing the expression levels between Col-0 and each genoype.

Fig. 3. Expression analysis of the *CHS, FLS, PAL1*, and *MYB12* genes.
(A) Table containing the AGI code, False Discovery Rate (FDR), and Fold Change (FC) for the genes from the Supplementary Datasets S1 and S2, color-coded for downregulation (blue). (B) and (C) Relative transcriptional levels of *CHS, FLS, PAL1*, and *MYB12* measured by qRT-PCR in root tissues of 5-day-old plants of Col-0*, d14, kai2*, *d14;kai2, max2* (B) or of *MYB12* in WT plants treated without (mock) and *rac*-GR24 for 6 h (C), and normalized to *ACT2, TUB2* and *PP2AA3*. Error bars represent the standard error (SE), based on three (B) and four (C) independent biological repeats. (B) One-way ANOVA with post hoc Dunnett test comparing the expression levels between Col-0 and each genotype ($P < 0.05$). (C) * $P < 0.05$, according to Student's *t* test. (D) Representative pictures of GUS staining of the 5-day-old *proMYB12::GUS* line grown in the presence of the 0.01% (v/v) acetone carrier or of 1 µM *rac*-GR24.

Fig. 4. Root response of *myb* mutants to *rac*-GR24.
(A) and (B) Equal volume of methanol extracts from the WT and the *myb11*,*myb111*,*myb12* triple mutant and from the WT, single, and double mutants for *myb11*, *myb12,* and *myb111* seedlings, grown without (mock) or with 1 µM *rac*-GR24, respectively, were spotted on HPTLC plates. DPBA staining followed by UV illumination was used to visualize flavonol glycosides; kaempferol derivatives (KD; blue) and quercetin derivatives (QD; orange). (C) *In planta* DPBA staining of the WT, single, and double mutants for *myb11*, *myb12*, and *myb111*.

Fig. 5. *rac*-GR24 responses of the *myb12* mutant.

(A) The *CHS*, *PAL1,* and *FLS1* expression in the root of Col-0 and the *myb12* mutant analyzed by qRT-PCR in 6-day-old plants grown in the presence of the 0.01% (v/v) acetone carrier or 1 µM *rac*-GR24 for 24 h and normalized to *ACT2*, *TUB2,* and *PP2AA3*. Error bars represent the standard error (SE), based on four independent biological repeats. Statistical grouping was determined by two-way ANOVA with post hoc Tukey test ($P < 0.05$). (B) Lateral root density (LRD) in 9-day-old WT and *myb12* seedlings grown on ½MS media with 1% (w/v) sucrose and in the presence of the 0.01% (v/v) acetone carrier (mock) or 1 µM *rac*-GR24. Six plants were measured per plate with six plates analyzed per line and per condition in each repeat ($n = 6$). Poisson regression model was used to define significant changes due to treatment for each genotype and differences in *rac*-GR24–induced LRD decrease between the genotypes, ***$P < 0.001$. (C) Root hair length of WT and *myb12* plants grown for 5 days on ½MS media with 1% (w/v) sucrose and in the presence of the 0.01% (v/v) acetone carrier or of 1 µM *rac*-GR24 with 25 plants measured per line and condition ($n = 25$). ***$P < 0.001$, *$P < 0.05$, according to a linear mixed model. Black asterisks indicate significant changes due to treatment, red asterisks, significant differences between genotypes in mock and asterisks above the line, differences in *rac*-GR24–induced root hair length increase between the genotypes. Representative images of the root hair phenotypes of the indicated genotypes. Scale bar, 0.5 mm.

Fig. 6. Expression and mutant analysis of the *HY5* gene.

(A) Table containing the AGI code, False Discovery Rate (FDR), and Fold Change (FC) for the genes from Supplementary Datasets S1 and S2, color-coded for upregulation (red) or downregulation (blue). (B) Relative transcriptional levels of *HY5* in Col-0, *d14*, *kai2*, *d14;kai2*, and *max2* mutants. RNA extracted from root tissue of 5-day-old plants analyzed by qRT-PCR as in Fig. 2B. (C) Lateral root density (LRD) of 9-day-old WT and *hy5* seedlings grown as described (Fig. 5B). Poisson regression model was used to define significant changes due to treatment for each genotype and differences in *rac*-GR24–induced LRD decrease between the genotypes (indicated above the line), ***$P < 0.001$; Six plants were measured per plate with six plates analyzed per line and per condition in each repeat ($n = 6$). (D) *In planta* DPBA staining of 5-day-old Col-0 and *hy5* plants grown on ½MS media with 1% (w/v) sucrose and in the presence of the 0.01% (v/v) acetone carrier (mock) or 1 µM *rac*-GR24 (GR24) under normal light (left) or upon UV excitation (right). (E) *MYB12* transcript levels detected through qRT-PCR of 5-day-old Col-0 and *hy5* plants analyzed as in Fig. 5A.

Fig. 7. Expression and mutant analysis of the *TMO5L1* gene.

(A) Table containing the AGI code, False Discovery Rate (FDR), and Fold Change (FC) of the genes from Supplementary Datasets S1 and S2, color-coded for upregulation (red) or downregulation (blue). Relative transcriptional levels of *TMO5L1* in Col-0*, d14, kai2*, *d14;kai2,* and *max2* mutants (B) and in Col-0 and *max2* plants after 6 h of treatment with 1 µM *rac*-GR24 or 0.01% (v/v) acetone (mock) (C). RNA was extracted from root tissue of 5-day-old plants and qRT-PCR was analyzed as in Fig. 2B. (B) One-way ANOVA with post hoc Dunnett test ($P < 0.05$) comparing the expression levels between Col-0 and each genotype. (C) Statistical grouping determined by two-way ANOVA with post hoc Tukey ($P < 0.05$). (D) Effect of 1 µM *rac*-GR24 on the LRD in Col-0 plants and *tmo5*, *tmo5 like1*, and *tmo5;tmo5like1* mutants after 9 days of growth. Data presented are means ± standard error (SE) of three biological repeats. Six plants were measured per plate with six plates analyzed per line and per condition in each repeat ($n = 6$). Poisson regression model was used to define

significant changes due to treatment for each genotype and differences in *rac*-GR24–induced LRD decrease between the genotypes (indicated above the line), *$P < 0.05$ and ***$P < 0.001$.

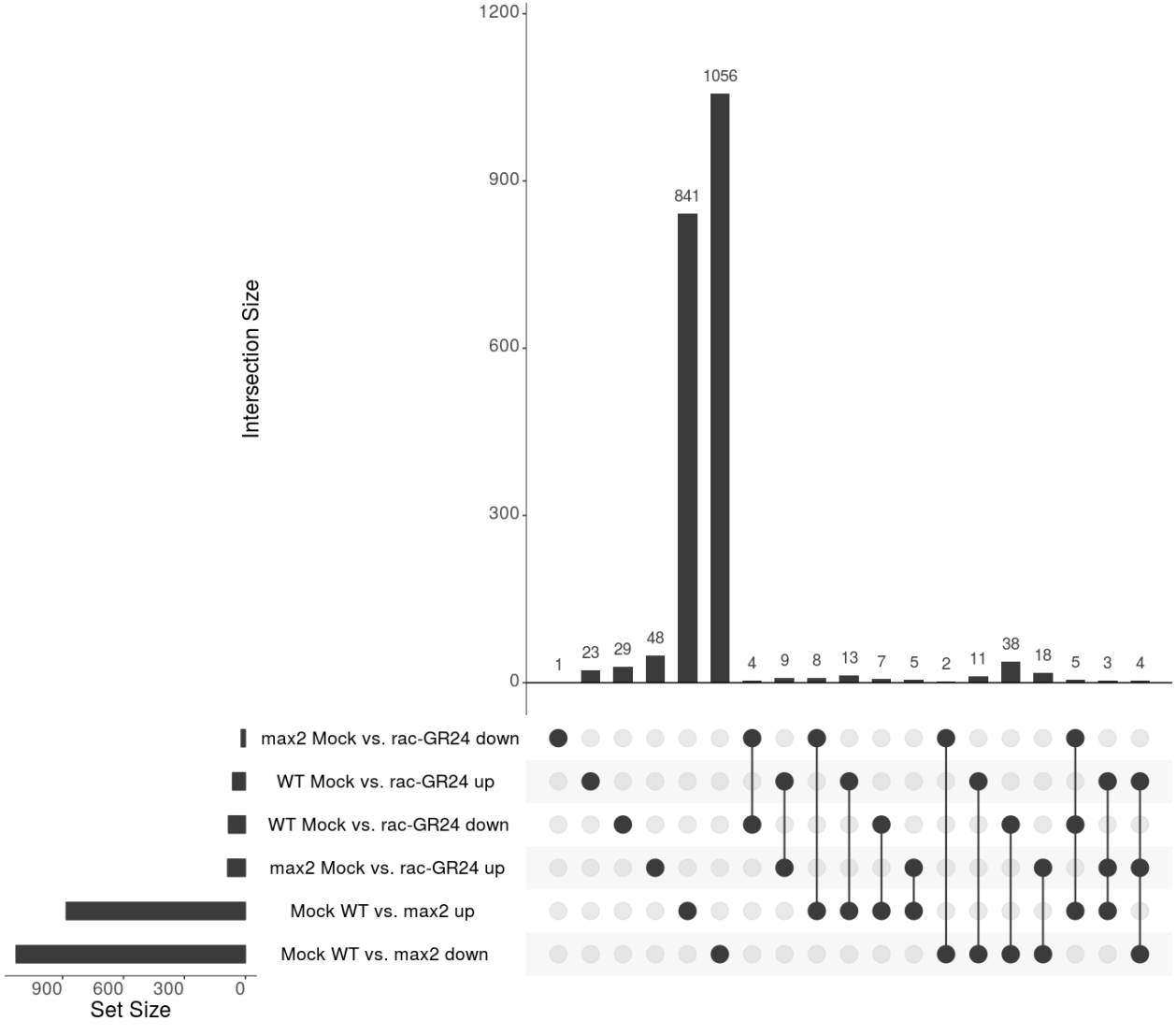
Intersection Size
1200
900
600
300
0
1
23
29
48
841
1056
4
9
8
13
7
5
2
11
38
18
5
3
4
max2 Mock vs. rac-GR24 down
WT Mock vs. rac-GR24 up
WT Mock vs. rac-GR24 down
max2 Mock vs. rac-GR24 up
Mock WT vs. max2 up
Mock WT vs. max2 down
900
600
300
0
Set Size

A

Description	AGI code	FDR (WT, Mock vs *rac*-GR24)	FC (WT, Mock vs *rac*-GR24)	FDR (Mock, WT vs *max2*	FC (Mock, WT vs *max2*
SMAX1	AT5G57710	0.990	0.984	2.54E-10	0.681
SMXL2	AT4G30350	0.0017	1.205	1.07E-62	0.452
SMXL7	AT2G29970	1.44E-12	1.447	2.07E-08	0.738

B

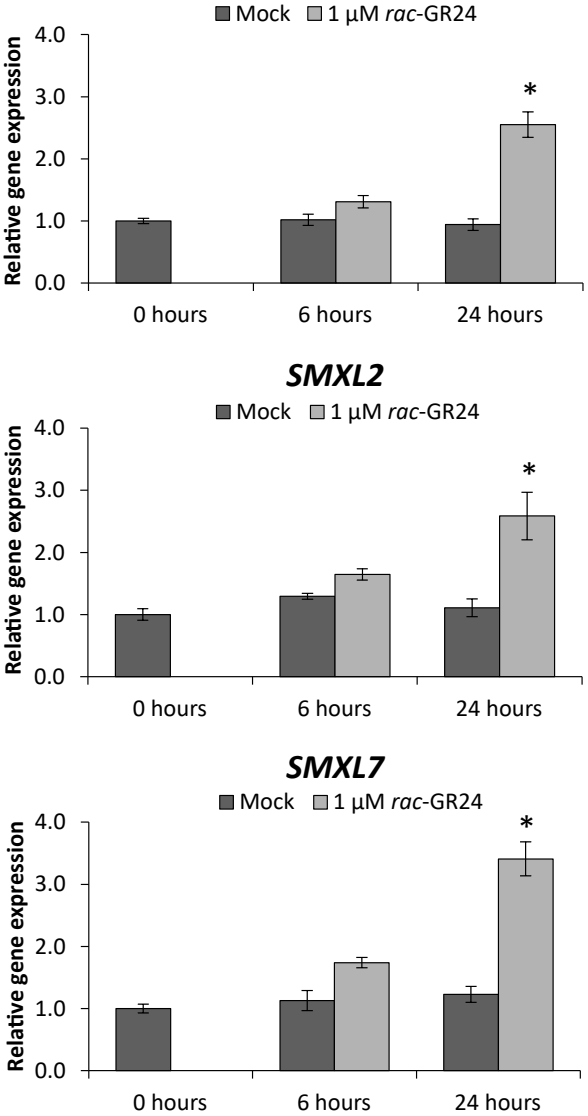

C

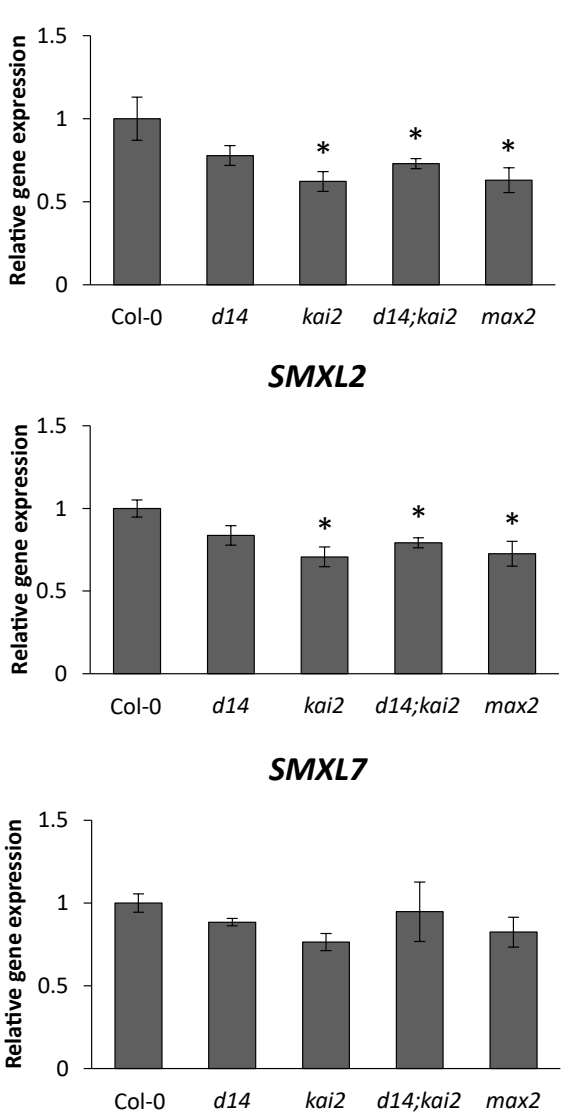

A

Description	AGI code	FDR (WT, Mock vs *rac*-GR24)	FC (WT, Mock vs *rac*-GR24)	FDR (Mock, WT vs *max2*)	FC (Mock, WT vs *max2*)
CHS	AT5G13930	0.729	1.055	3E-110	0.379
PAL1	AT2G37040	0.997	0.998	5.11E-38	0.584
FLS1	AT5G08640	0.656	1.075	5.21E-78	0.390
MYB12	AT2G47460	0.224	1.117	7.08E-41	0.539

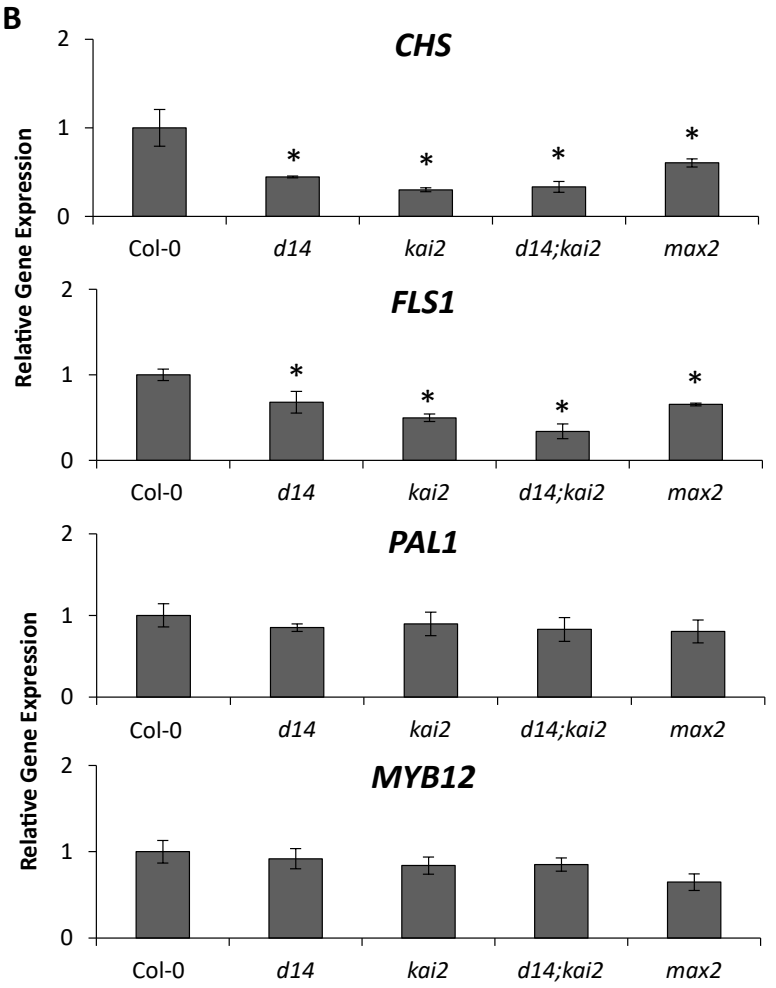

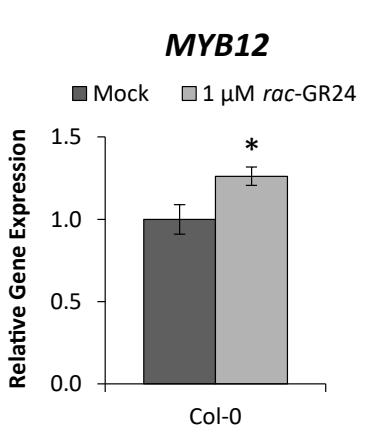

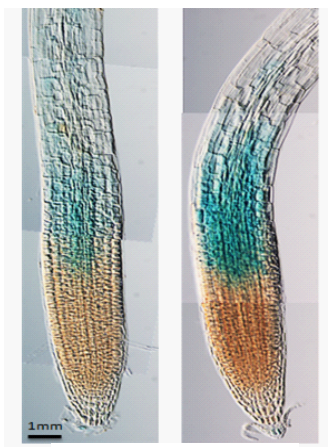

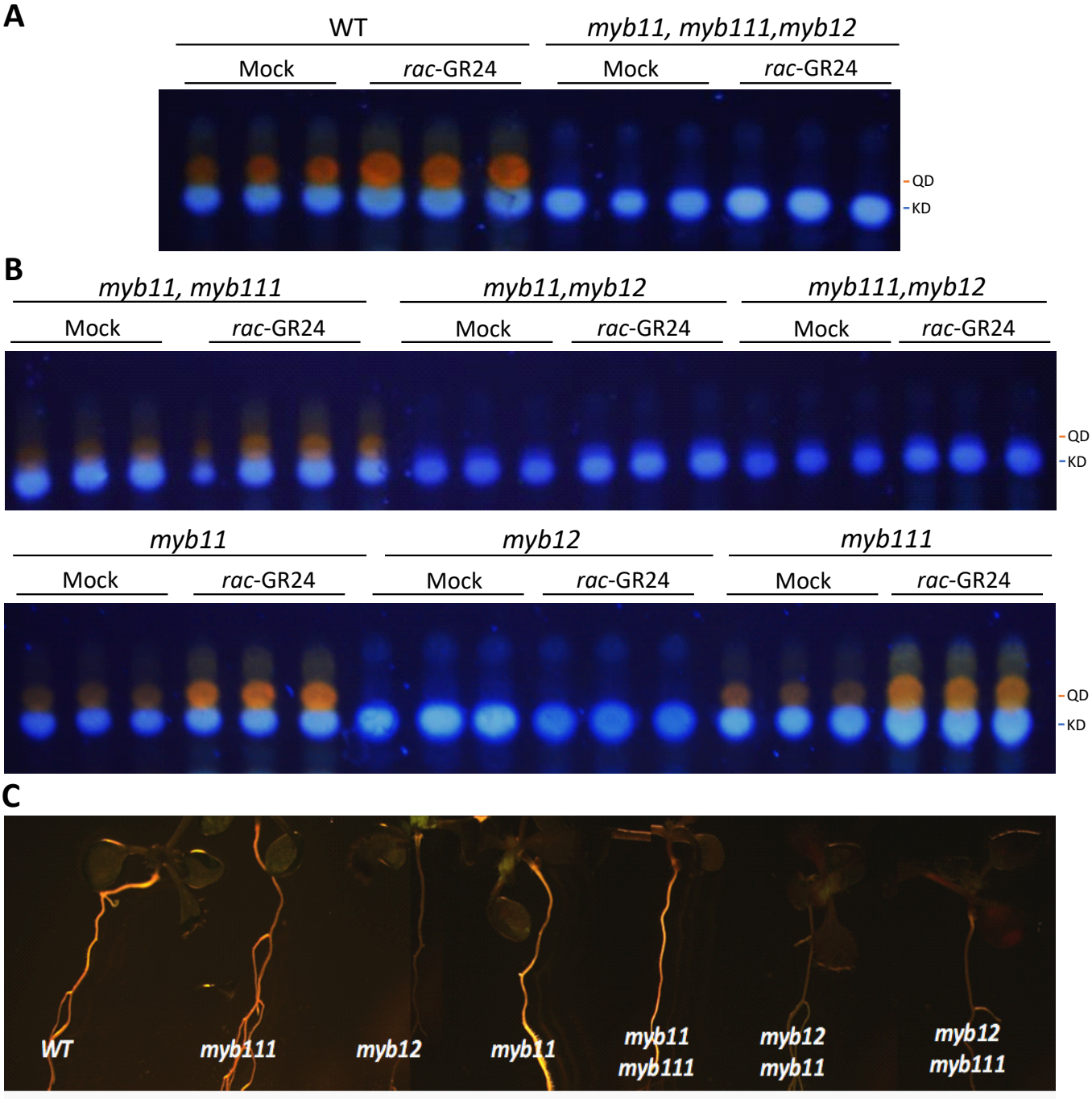
A
WT
myb11, myb111,myb12
Mock
rac-GR24
Mock
rac-GR24
QD
KD
B
myb11, myb111
myb11,myb12
myb111,myb12
Mock
rac-GR24
Mock
rac-GR24
Mock
rac-GR24
QD
KD
myb11
myb12
myb111
Mock
rac-GR24
Mock
rac-GR24
Mock
rac-GR24
QD
KD
C
WT
myb111
myb12
myb11
myb11
myb111
myb12
myb11
myb12
myb111

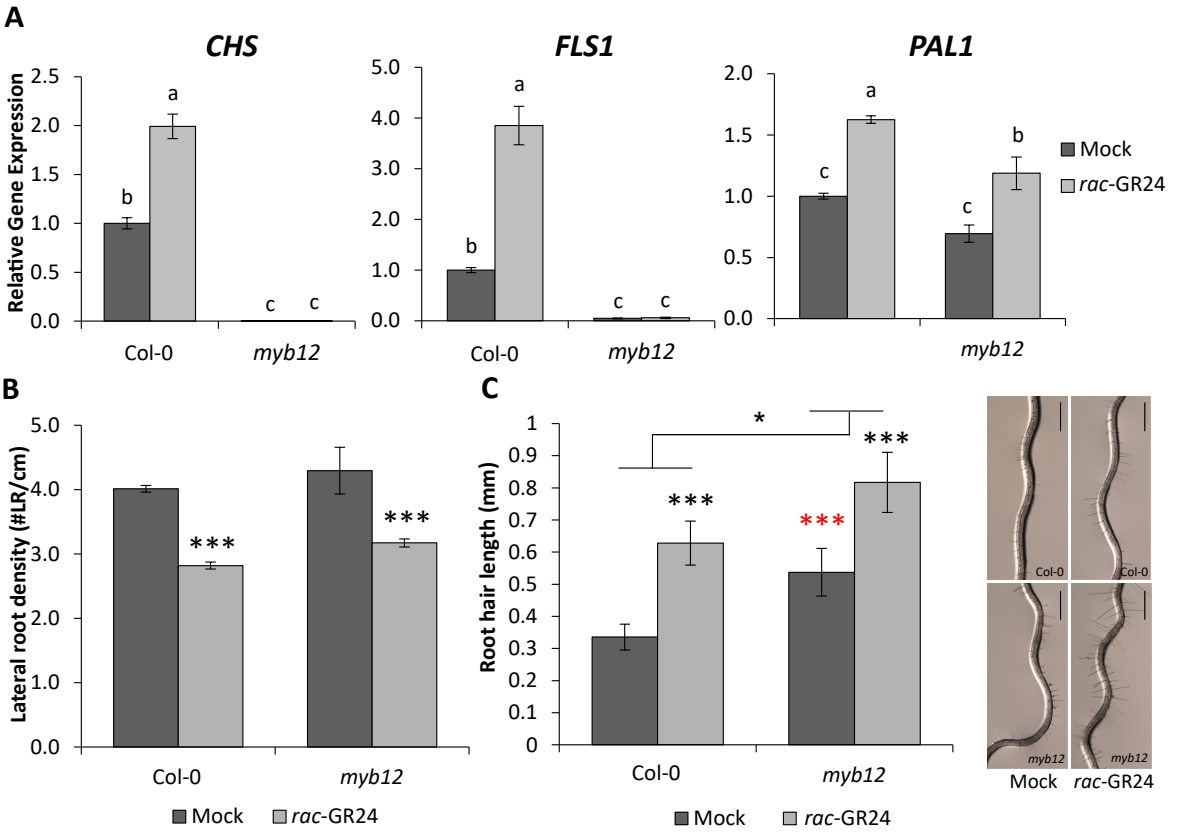
A
CHS
FLS1
PAL1
Relative Gene Expression
Col-0
myb12
Mock
rac-GR24
B
Lateral root density (#LR/cm)
C
Root hair length (mm)
Mock
rac-GR24

A

Description	AGI code	FDR (WT, Mock vs *rac*-GR24)	FC (WT, Mock vs *rac*-GR24)	FDR (Mock, WT vs *max2*)	FC (Mock, WT vs *max2*)
HY5	AT5G11260	0.949	0.983	1.84E-08	0.772
HYH	AT3G17609	0.976	0.985	7.52E-07	0.720

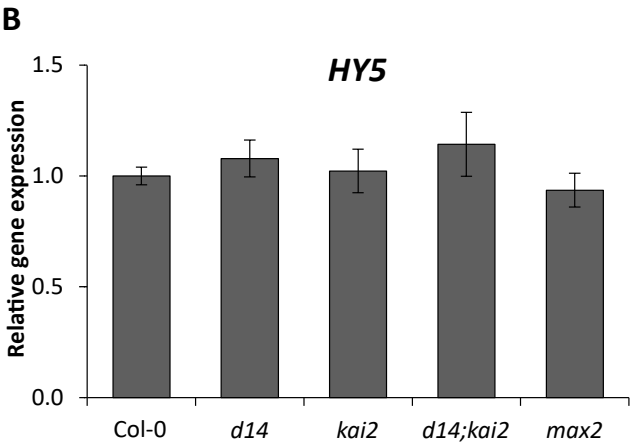

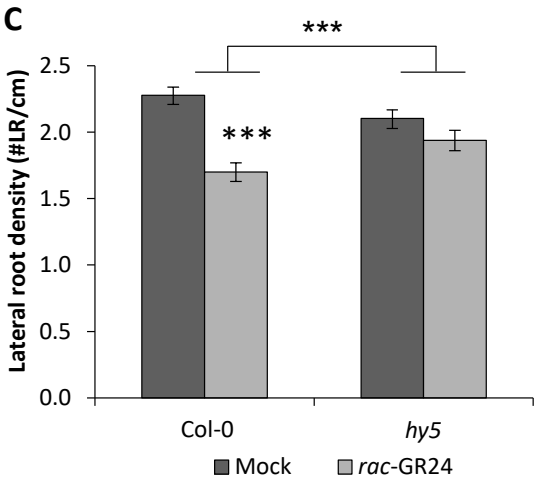

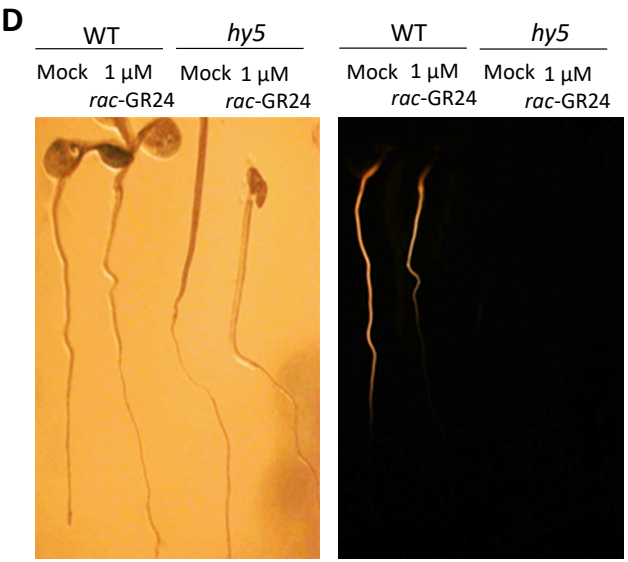

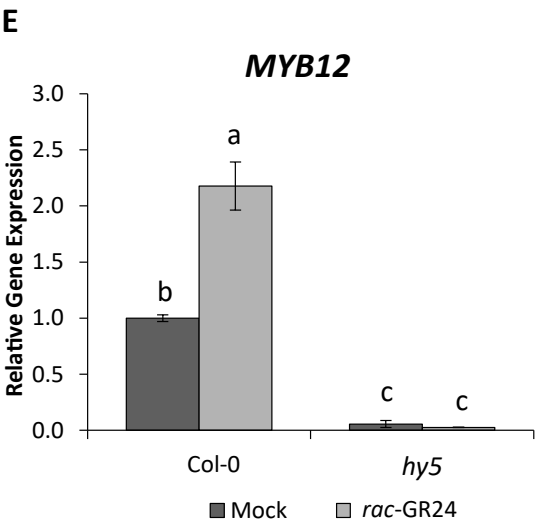

A

Description	AGI code	FDR (WT, Mock vs *rac*-GR24)	FC (WT, Mock vs *rac*-GR24)	FDR (Mock, WT vs *max2*)	FC (Mock, WT vs *max2*)
TMO5L1	AT1G68810	6.85E-27	0.487179	6.65E-06	1.308952
TMO5	AT3G25710	0.023417	0.793934	0.001548	1.245593